Hindawi Publishing Corporation
Journal of Applied Mathematics
Volume 2008, Article ID 586567, 40 pages
doi:10.1155/2008/586567

Research Article

Velocity Induced by a Plane Uniform Vortex Having the Schwarz Function of Its Boundary with Two Simple Poles

G. Riccardi and D. Durante

Department of Aerospace and Mechanical Engineering, Second University of Naples, Via Roma 29, Aversa, 81031 Caserta, Italy

Correspondence should be addressed to G. Riccardi, giorgio.riccardi@email.it

Received 6 June 2008; Accepted 8 September 2008

Recommended by Bernard Geurts

The velocity induced by a plane, uniform vortex is investigated through the use of an integral relation between Schwarz function of the vortex boundary and conjugate of the velocity. The analysis is restricted to a certain class of vortices, the boundaries of which are described through conformal maps onto the unit circle and the corresponding Schwarz functions possess two poles in the plane of the circle. The dependence of the velocity field on the vortex shape is investigated by comparing velocity and streamfunction with the ones of the equivalent Rankine vortex (which has the same vorticity, area, and center of vorticity). By changing the parameters of the Schwarz function (poles and corresponding residues), rather complicated vortex shapes can be easily analyzed, some of them mimicing an incipient filamentation of the vortex boundary.

1. Introduction

The present paper investigates the self-induced velocity field of a uniform vortex having Schwarz function of its boundary with two simple poles on a suitable transformed plane. This analysis is viewed as a first step towards the study of the dynamics of such a vortex in terms of the related Schwarz function.

The use of the Schwarz function in searching vortex equilibria and also in investigating their stability properties dates back to the eighties of the last century (e.g., see the elegant discussion in [1, Section 9.2]). As well known, the Schwarz function $\mathbf{\Phi}(\mathbf{x})$ of an analytic curve $\mathcal{L}$ in the plane of the complex variable $x_1 + \mathbf{i}x_2 = \mathrm{Re}(\mathbf{x}) + \mathbf{i}\,\mathrm{Im}(\mathbf{x}) = \mathbf{x}$ satisfies the request $\mathbf{\Phi}(\mathbf{x}) := x_1 - \mathbf{i}x_2 = \overline{\mathbf{x}}$ (a definition is indicated by joining the two symbols ":" and "=", with the first one on the side in which the new quantity appears) in any point $\mathbf{x} \in \mathcal{L}$ and is defined via analytic continuation on a suitable neighbourhood of the curve $\mathcal{L}$. In general, singularities of

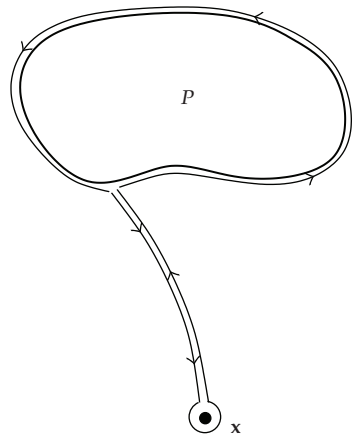

Figure 1: Integration path for studying the asymptotic behavior of the function $\mathbf{G}(\mathbf{x})$.

the function $\mathbf{\Phi}$ are found inside and outside $\mathcal{L}$. An extensive theoretical background on the Schwarz function can be found in [2], while an attempt to summarize the original ideas on the use of such a function in searching vortex equilibria may be the following one.

The curve $\mathcal{L}$ is taken as the boundary ∂P of a uniform vortex P (with unitary vorticity, for the sake of simplicity) and it is assumed that $\mathbf{\Phi}$ can be rewritten as the sum of two functions: $\mathbf{\Phi} = \mathbf{F} + \mathbf{G}$, where $\mathbf{F}$ and $\mathbf{G}$ are analytic inside and outside ∂P, respectively. It is worth noticing that the behavior of $\mathbf{G}(\mathbf{x})$ for $\mathbf{x} \to \infty$ follows just from the above splitting of $\mathbf{\Phi}$. Indeed, consider the integral on the path of Figure 1 of the function $\mathbf{G}(\mathbf{y})/[2\pi\mathbf{i}(\mathbf{x}-\mathbf{y})]$, for $\mathbf{x}$ fixed away from the vortex. It gives the value of $\mathbf{G}(\mathbf{x})$ in terms of the moments of the Schwarz function:

$$\mathbf{G}(\mathbf{x}) = \frac{1}{2\pi\mathbf{i}}\int_{\partial P} d\mathbf{y}\frac{\mathbf{G}(\mathbf{y})}{\mathbf{x}-\mathbf{y}} = \frac{1}{2\pi\mathbf{i}}\int_{\partial P} d\mathbf{y}\frac{\mathbf{\Phi}(\mathbf{y})}{\mathbf{x}-\mathbf{y}} = \sum_{k=0}^{\infty}\frac{1}{\mathbf{x}^{k+1}}\cdot\frac{1}{2\pi\mathbf{i}}\int_{\partial P} d\mathbf{y}\,\mathbf{y}^{k}\mathbf{\Phi}(\mathbf{y}), \tag{1.1}$$

with the integral having $\mathbf{F}$ in place of $\mathbf{G}$ vanishing, because $\mathbf{F}$ is analytic inside P. By accounting for that the integral for $k = 0$ gives $2\mathbf{i}$ times the area $|P|$ of the vortex, the asymptotic behavior of $\mathbf{G}$ follows as $\mathbf{G}(\mathbf{x}) \sim |P|/(\pi\mathbf{x})$.

It can be noticed that the conjugate of the velocity $\overline{\mathbf{u}}$ is analytic outside P, while $\overline{\mathbf{u}} - \overline{\mathbf{x}}/(2\mathbf{i})$ is analytic inside the vortex (both cases will be unified in terms of a Cauchy integral of $\mathbf{\Phi}$ in (2.9) below); it follows that $\overline{\mathbf{u}}$ must have the form

$$\overline{\mathbf{u}}(\mathbf{x}) = \begin{cases} \dfrac{\overline{\mathbf{x}} - \mathbf{F}(\mathbf{x})}{2i} & \text{inside } P, \\ \dfrac{\mathbf{G}(\mathbf{x})}{2i} & \text{outside } P. \end{cases} \tag{1.2}$$

Indeed, the continuity across the vortex boundary follows by that $\mathbf{G} = \overline{\mathbf{x}} - \mathbf{F}$ on the ∂P, $\overline{\mathbf{u}}$ behaves at infinity as $|P|/(2\pi\mathbf{i}\mathbf{x})$, and the corresponding vorticity is uniform and unitary inside P and vanishes outside. At this stage, it is also easy to show that the asymptotic behavior of the velocity is related to the (complex) moments of the Schwarz function, through the power series of $1/\mathbf{x}$ (1.1).

The formula (1.2) relates velocity and Schwarz function in a very appealing way. However, the identification of the functions **F** and **G** is often a quite complicated goal, which is reached by firstly identifying **G** through its asymptotic behavior (1.1) and then by taking **F** as $\mathbf{\Phi} - \mathbf{G}$. In the present paper, an approach which is alternative to the use of the relation (1.2) is proposed: $\overline{\mathbf{u}}$ and $\mathbf{\Phi}$ are related through a Cauchy integral, which is evaluated without splitting the Schwarz function. The two approaches are completely equivalent: if the Schwarz function is not too complicated, the splitting (1.2) is still more convenient, but in other cases the present approach can give some advantage. As an important example, for the class of vortices investigated in the present paper the use of the integral approach results in being much easier than the one of the splitting (1.2).

When the shape of the uniform vortex P is not far from a circular one (*quasicircular* vortex), the identification of **F** and **G** is rather simple and the analysis can go ahead [3]. The vortex boundary belongs to a ring inside which the Schwarz function is evaluated via a Laurent series, with **F** and **G** being the analytic continuations of its regular and singular parts, respectively. Due to the small differences from a circle, it is also convenient to use a Laurent series in order to define the vortex shape through a conformal map between the unit circle and ∂P. The coefficients of the series for $\mathbf{\Phi}$ are nonlinear combinations of the ones of the map. Configurations of absolute equilibrium in presence of external rotation and stationary strain (intensity and principal axes of which are kept fixed in time) have been investigated by imposing that the normal velocity of the fluid at the vortex boundary vanishes: $\mathbf{u}\partial_{\mathbf{z}}\overline{\mathbf{x}} \equiv \overline{\mathbf{u}}\partial_{\mathbf{z}}\mathbf{x}$. This relation is enforced to be identically satisfied in $\mathbf{z}$, that is, any power of $\mathbf{z}$ is multiplied times a vanishing coefficient: a nonlinear system in the map coefficients follows, to which conditions concerning the area of the vortex and the position of its center of vorticity are added. The system is numerically solved via a multidimensional Newton solver. Finally, the linear stability of stationary solutions also is investigated with the above approach. The coefficients of the conformal map are taken as functions of time, and it is enforced that the normal components of the velocity of the fluid and of the vortex boundary agree: $(\partial_t\mathbf{x} - \mathbf{u})\partial_{\mathbf{z}}\overline{\mathbf{x}} \equiv (\partial_t\overline{\mathbf{x}} - \overline{\mathbf{u}})\partial_{\mathbf{z}}\mathbf{x}$. The above constraint is linearized around a stationary solution, time dependence is fixed in the form $\exp(\boldsymbol{\sigma} t)$ (with $\boldsymbol{\sigma}$ being a complex number, the real part of which determines the stability properties of the vortex) and an eigenvalue problem is deduced. Several interesting cases of bifurcations of equilibria are discussed, with particular regard to the energy conservation. Also the dynamics of quasicircular vortices has been investigated [4], but by using a quite different approach. The vortex boundary is described in terms of a Fourier series and an equation of evolution for the Fourier coefficients is deduced. It is also found that the derivatives along the vortex boundary of the velocity and of the Schwarz function are related through a Cauchy integral.

In the last ten years, a large research activity has been devoted to find and analyze stationary solutions of the Euler equation by using the Schwarz function. The vortex shape is searched by starting from the following form of the streamfunction ψ_r in a corotating frame of reference:

$$\psi_r(\mathbf{x}) \propto \mathbf{x}\overline{\mathbf{x}} - \int^{\mathbf{x}} d\mathbf{y}\mathbf{\Phi}(\mathbf{y}) - \int^{\overline{\mathbf{x}}} d\mathbf{y}\overline{\mathbf{\Phi}}(\mathbf{y}). \tag{1.3}$$

The form (1.3) is assumed valid outside or inside the vortex, while ψ_r is taken as vanishing on the complementary part of the physical plane. Multipolar equilibria have been analyzed in [5], where symmetrical configurations of point vortices are placed into a uniform one, in such a way that the total circulation vanishes. In this paper, the form (1.3) is built as

an extension to general shapes of the streamfunction for the shielded Rankine vortex (see also [6], in which the discussion is carried out in the framework of the quadrature domains by using a fundamental theorem of Aharonov and Shapiro). The stability properties of the above equilibria have been analyzed in [7], both in the framework of a linear theory and through fully nonlinear numerical simulations with a contour dynamics approach (see (2.2) below). Quadrupoles, pentapoles, and higher have been found to be stable equilibria, while the tripoles result in being linearly unstable. Other interesting equilibria involving a doubly connected uniform vortex and an internal set of pointwise ones are found in [8], mimicing the overlapping of shielded Rankine vortices. An irrotational region remains trapped at the center of the vortex. In [9], a class of stationary solutions consisting in a uniform vortex surrounded by a certain number of point corotating vortices placed on the vertices of a regular polygon is built and analyzed. This vortex pattern depends on an integer number N, which specifies the number of satellite vortices, and on a parameter a belonging to a lower bounded interval of the real axis. In correspondence to the minimum value of a and for a given N, called $a_{\text{crit}}^{(N)}$, the central uniform vortex exhibits a nonanalytic boundary in which N cusps are present. For growing $a > a_{\text{crit}}^{(N)}$, the central uniform vortex becomes smaller and smaller (its area decreasing as $1/a^2$), with its shape going to a circular one. In [10], the streamfunction (1.3) is used to generalize to finite-area vortices the ideas of Aref and Vainchtein [11] who search asymmetric equilibria of point vortices by inserting new vortices on points of relative rest (in a corotating reference frame). By such an approach, growing uniform vortices are inserted in a corotating vortex pair until the Rankine vortex is reached. The stability of such one-parameter family of equilibria has been also tested through numerical simulations with a contour dynamics approach. Other equilibria depending on two parameters and involving uniform vortices and point vortices are found in [12], still starting from the streamfunction (1.3). A central uniform vortex is surrounded by an alternate distribution of pointwise and uniform vortices. Also in this case, vortex shapes with cusps are found for certain critical values of the parameters and numerical simulations show the formation of filaments in configurations having large satellite vortices with cusps, as well as in perturbed (by displacing point vortices) equilibria.

The present paper deals with the self-induced velocity of any vortex, the boundary of which possesses a Schwarz function with two simple poles (on a suitable transformed plane). This vortex shape appears to be the simplest, but nontrivial, possible one: the velocity can be evaluated analytically by using an integral link with the corresponding function $\mathbf{\Phi}$ of its boundary. For this reason, it has been selected by the authors as the starting point of an analysis of the vortex motion through the dynamics of $\mathbf{\Phi}$, which satisfies the evolution equation [13]:

$$\partial_t \mathbf{\Phi} = \overline{\mathbf{u}} - \mathbf{u}\partial_x \mathbf{\Phi}. \tag{1.4}$$

In order to investigate nontrivial sample cases, the analytical forms of the velocity are needed in (1.4). The present analysis achieves the first step of such a way. At the same time, it shows the advantage of using an integral link between $\mathbf{\Phi}$ and $\overline{\mathbf{u}}$.

The paper is organized as follows. The integral relation between Schwarz function and velocity is presented in Section 2. In Section 3, an overall view of the geometrical properties of the vortices having Schwarz function with two simple poles is given. A classification of this kind of vortices is proposed in Section 4, while a discussion of several sample cases follows in Section 5. In Section 6, the inverse map (from the physical plane to the transformed one)

is built and the self-induced velocity is analytically evaluated. The different velocity fields (together with the corresponding streamfunctions) are shown and discussed in Section 7, where we also propose the use of an equivalent Rankine vortex in order to investigate the dependence of the velocity on the vortex shape. Conclusions are offered in Section 8, together with a sketch of the principal research lines under investigation at the present time.

2. An integral relation between Schwarz function and velocity

The velocity induced by a uniform vortex P (inside which the vorticity is unitary, for the sake of simplicity) depends only on the shape of its boundary ∂P: if it is smooth and its length is finite, then in any point $\mathbf{x}$ of the plane the velocity is given by

$$\mathbf{u}(\mathbf{x}) = -\int_{\partial P} d\mathbf{y} G(\mathbf{x}-\mathbf{y}), \tag{2.1}$$

where G is the Green function of the Laplace operator, that is, $G(\mathbf{x}) = (\log x)/(2\pi)$ (the modulus of a vector is represented with the same symbol, but without using the bold character, e.g., $x = |\mathbf{x}| = (x_1^2 + x_2^2)^{1/2}$), and $d\mathbf{y}$ is the curve element. The motion of such a kind of vortex is defined by the time evolution of its boundary, starting from a smooth and finite-length boundary at the initial time ($t = 0$). In order to numerically investigate that motion, the form (2.1) of the velocity is used as briefly described below.

Consider a parameter σ_t on ∂P at time t. With the vortex motion being a material one, it is possible to write σ_t as a function of the corresponding parameter σ_0 at the initial time ($t = 0$) and of the time t itself: $\sigma_t = \sigma_t(\sigma_0, t)$. The Lagrangian representation of the position on the vortex boundary $\mathbf{x} = \mathbf{x}[\sigma_t(\sigma_0, t), t] = \mathbf{x}^{(\mathcal{L})}(\sigma_0, t)$ becomes natural and the velocity (2.1) evaluated on that point, that is $\mathbf{u}[\mathbf{x}^{(\mathcal{L})}(\sigma_0, t)]$, gives the Lagrangian velocity $\partial_t \mathbf{x}^{(\mathcal{L})}(\sigma_0, t)$. It follows that the motion of ∂P is the solution of the Cauchy problem:

$$\begin{gathered} \partial_t \mathbf{x}^{(\mathcal{L})}(\sigma_0, t) = \mathbf{u}\left[\mathbf{x}^{(\mathcal{L})}(\sigma_0, t)\right], \\ \mathbf{x}^{(\mathcal{L})}(\sigma_0, 0) \text{ given.} \end{gathered} \tag{2.2}$$

The above approach is known as *contour dynamics* [14, 15], a powerful tool to investigate the inviscid, incompressible two-dimensional vortex motion. Obviously, in the numerical practice a certain number of nodes are selected on the initial boundary and their motion is followed in time. In the discrete framework, the velocity (2.1) is evaluated through an interpolation procedure which rebuilds an approximation of ∂P.

By starting from the contour dynamics form of the velocity (2.1), in the present section an integral relation between Schwarz function and velocity is deduced, which is equivalent to the form (1.2) but it does not require the splitting of the Schwarz function in the sum $\mathbf{F}+\mathbf{G}$. The key observation about (2.1) lies in considering that if the point $\mathbf{x}$ is not on the vortex boundary, an integration by parts enables us to write

$$\mathbf{u} = -\frac{1}{2\pi}\int_{\partial P} \frac{(\mathbf{x}-\mathbf{y})\cdot d\mathbf{y}}{|\mathbf{x}-\mathbf{y}|^2}\mathbf{y}, \tag{2.3}$$

with the dot indicating a scalar product. By conjugating both sides of the above relation, it may be rewritten in the following complex form:

$$\overline{\mathbf{u}} = \frac{1}{2\mathbf{i}}\left[\overline{\frac{1}{2\pi\mathbf{i}}\int_{\partial P}\frac{d\mathbf{y}}{\mathbf{y}-\mathbf{x}}}\,\overline{\mathbf{x}} + \frac{1}{2\pi\mathbf{i}}\int_{\partial P} d\mathbf{y}\frac{\boldsymbol{\Phi}(\mathbf{y})}{\mathbf{x}-\mathbf{y}}\right]. \tag{2.4}$$

Notice that the first integral in the right-hand side of the above equation holds 1 if $\mathbf{x}$ lies inside the vortex ($\mathbf{x} \in \mathring{P}$), while it vanishes when $\mathbf{x}$ is external to the vortex ($\mathbf{x} \in P'$). Equation (2.4) relates velocity and Schwarz function in any point $\mathbf{x}$ which does not lie on the vortex boundary, while if the point $\mathbf{x}$ belongs to that curve, the discussion must be carried out in a more sophisticated way.

The tangent derivative of the conjugate of the velocity on the vortex boundary ∂P has been investigated in a previous paper [4], where it has been shown that it is related to the tangent derivative of the Schwarz function, that is, to the function $\boldsymbol{\phi} := \boldsymbol{\Phi}' = 1/\boldsymbol{\tau}^2$, with $\boldsymbol{\tau}$ being the unit vector which is tangent to ∂P. The relation is through a Cauchy integral (see [4, equation (18)], rewritten here for reader's convenience):

$$\partial_{\mathbf{x}}\overline{\mathbf{u}}(\mathbf{x}) = \frac{1}{2\mathbf{i}}\left[\frac{1}{2}\boldsymbol{\phi}(\mathbf{x}) + \frac{1}{2\pi\mathbf{i}}\int_{\partial P} d\mathbf{y}\frac{\boldsymbol{\phi}(\mathbf{y})}{\mathbf{x}-\mathbf{y}}\right] =: \frac{1}{2\mathbf{i}}\mathbf{V}(\mathbf{x}). \tag{2.5}$$

By changing $\boldsymbol{\phi}(\mathbf{y})$ with $-\partial_{\mathbf{y}}(\overline{\mathbf{x}}-\overline{\mathbf{y}})$, an integration by parts gives

$$\begin{aligned}\mathbf{V} &= \frac{1}{2\pi\mathbf{i}}\int_{\partial P} d\mathbf{y}\frac{\overline{\mathbf{x}}-\overline{\mathbf{y}}}{(\mathbf{x}-\mathbf{y})^2} + \frac{1}{2}\boldsymbol{\phi}(\mathbf{x}) \\ &= -\frac{d}{d\mathbf{x}}\frac{1}{2\pi\mathbf{i}}\int_{\partial P} d\mathbf{y}\frac{\overline{\mathbf{x}}-\overline{\mathbf{y}}}{\mathbf{x}-\mathbf{y}} + \frac{\boldsymbol{\phi}(\mathbf{x})}{2\pi\mathbf{i}}\int_{\partial P}\frac{d\mathbf{y}}{\mathbf{x}-\mathbf{y}} + \frac{1}{2}\boldsymbol{\phi}(\mathbf{x}),\end{aligned} \tag{2.6}$$

in which the second integral in the last side holds $-\pi\mathbf{i}$, it follows that

$$\mathbf{V} = \frac{d}{d\mathbf{x}}\left[\frac{1}{2}\boldsymbol{\Phi}(\mathbf{x}) + \frac{1}{2\pi\mathbf{i}}\int_{\partial P} d\mathbf{y}\frac{\boldsymbol{\Phi}(\mathbf{y})}{\mathbf{x}-\mathbf{y}}\right]. \tag{2.7}$$

In this way, the conjugate of the velocity in the point $\mathbf{x}$ belonging to the patch boundary becomes

$$\overline{\mathbf{u}} = \frac{1}{2\mathbf{i}}\left[\frac{1}{2}\boldsymbol{\Phi} + \frac{1}{2\pi\mathbf{i}}\int_{\partial P} d\mathbf{y}\frac{\boldsymbol{\Phi}(\mathbf{y})}{\mathbf{x}-\mathbf{y}}\right]. \tag{2.8}$$

Equations (2.4) and (2.8) are summarized by introducing the characteristic function of the domain P : $\chi_P : C \to \{0, 1/2, 1\}$, which holds 1 inside P, 0 outside P, and $1/2$ on the boundary, in the following new form of the self-induced velocity:

$$\overline{\mathbf{u}}(\mathbf{x}, \overline{\mathbf{x}}) = \frac{1}{2\mathbf{i}}\left[\chi_P(\mathbf{x})\overline{\mathbf{x}} + \frac{1}{2\pi\mathbf{i}}\int_{\partial P} d\mathbf{y}\frac{\boldsymbol{\Phi}(\mathbf{y})}{\mathbf{x}-\mathbf{y}}\right], \tag{2.9}$$

with the position that the integral must be a Cauchy one if the point $\mathbf{x}$ lies on the curve ∂P. It is worth noticing that the velocity (2.9) is a function of both $\mathbf{x}$ and $\overline{\mathbf{x}}$ inside the vortex, while it depends on $\mathbf{x}$ only on ∂P (through the Schwarz function) and outside the vortex. The velocity (2.9) is a continuous function across ∂P: indeed if $\mathbf{x}$ approaches $\mathbf{x}_0 \in \partial P$ from the inside of the vortex, $\chi_P(\mathbf{x})\overline{\mathbf{x}}$ goes to $\overline{\mathbf{x}}_0$ and the integral to $-\overline{\mathbf{x}}_0$ plus continuous terms (given by the singularities of the Schwarz function), while if $\mathbf{x}$ reaches $\mathbf{x}_0$ from the outside, the first term vanishes and only the above continuous contribution remains. On the vortex boundary, $\chi_P(\mathbf{x})\overline{\mathbf{x}}$ holds $\overline{\mathbf{x}}_0/2$, while the integral must be considered as Cauchy's one and it leads to a contribution $-\overline{\mathbf{x}}_0/2$ plus the continuous contribution due to the singularities of $\mathbf{\Phi}$. The above form of the velocity gives also the correct asymptotic behavior: $\overline{\mathbf{u}}(\mathbf{x}) \sim |P|/(2\pi\mathbf{i}\mathbf{x})$ for $\mathbf{x}$ going to infinity, $|P|$ being the area of the vortex. It is also important to notice that once the splitting $\mathbf{\Phi} = \mathbf{F} + \mathbf{G}$ is inserted into the integral at the right-hand side of (2.9), the original formulation (1.2) is recovered.

As a first sample case for the use of (2.9), consider an elliptical vortex having center of vorticity on the origin and semiaxes a along x_1 and b ($< a$) along x_2 (the related quantities $c = \sqrt{a^2 - b^2}$, $\delta = (a^2+b^2)/c^2$, $\chi = 2ab/c^2$, and $\mu = (a-b)/(a+b) < 1$ will be also used below). By using the angle $\theta \in [0, 2\pi)$, the curve ∂P is parametrized as $\mathbf{x}(\theta) = a\cos\theta + \mathbf{i}b\sin\theta$, which is rewritten in terms of $\mathbf{z} = \exp(\mathbf{i}\theta)$ as

$$\mathbf{x}(\mathbf{z}) = \frac{a+b}{2}\left(\mathbf{z} + \frac{\mu}{\mathbf{z}}\right). \tag{2.10}$$

Equation (2.10) defines a conformal map between the plane of the unit circle ($\mathbf{z}$) and the physical one ($\mathbf{x}$). Due to the fact that the ellipse is a simple curve, the equation in $\boldsymbol{\zeta}$: $\mathbf{x}(\mathbf{z}) = \mathbf{x}(\boldsymbol{\zeta})$ cannot have another solution on $\mathcal{C}$ unless $\boldsymbol{\zeta} = \mathbf{z}$. Indeed, it also possesses the solution $\boldsymbol{\zeta} = \boldsymbol{\zeta}^\star(\mathbf{z}) = \mu/\mathbf{z}$ (notice that $\boldsymbol{\zeta}^\star[\boldsymbol{\zeta}^\star(\mathbf{z})] = \mathbf{z}$). The solutions $\mathbf{z}$ and $\boldsymbol{\zeta}^\star$ are expressed in terms of $\mathbf{x}$ in the following way:

$$\begin{aligned} \mathbf{z}(\mathbf{x}) &= \frac{\left(\sqrt{\mathbf{x}+c} + \sqrt{\mathbf{x}-c}\right)^2}{2(a+b)}, \\ \mathbf{z}^\star(\mathbf{x}) := \boldsymbol{\zeta}^\star[\mathbf{z}(\mathbf{x})] &= \frac{\left(\sqrt{\mathbf{x}+c} - \sqrt{\mathbf{x}-c}\right)^2}{2(a+b)}. \end{aligned} \tag{2.11}$$

If the point $\mathbf{x}$ belongs to the vortex, then $\mu < z < 1$ and the same holds also for $z^\star$, while for $\mathbf{x} \in P'$, $\mathbf{z}$ lies outside the unit circle and $z^\star < \mu$. By conjugating both sides of (2.10) for $\mathbf{z} \in \mathcal{C}$, the Schwarz function follows naturally as the function of $\mathbf{z}$:

$$\mathbf{\Phi}(\mathbf{z}) = \frac{a+b}{2}\left(\mu\mathbf{z} + \frac{1}{\mathbf{z}}\right). \tag{2.12}$$

The velocity is evaluated by rewriting (2.9) in the transformed plane $\mathbf{z}$:

$$\overline{\mathbf{u}} = \frac{1}{2\mathbf{i}}\left[\chi_P(\mathbf{x})\overline{\mathbf{x}} - \frac{1}{2\pi\mathbf{i}}\frac{a+b}{2}\int_{\mathcal{C}} d\boldsymbol{\zeta}\frac{\left(\boldsymbol{\zeta}^2 - \mu\right)\left(\mu\boldsymbol{\zeta}^2 + 1\right)}{\boldsymbol{\zeta}^2(\boldsymbol{\zeta} - \mathbf{z})(\boldsymbol{\zeta} - \mathbf{z}^\star)}\right]. \tag{2.13}$$

If $\mathbf{x} \in \mathring{P}$, then both poles $\mathbf{z}$ and $\mathbf{z}^\star$ are internal to $\mathcal{C}$ and the above equation gives

$$\overline{\mathbf{u}}(\mathbf{x}, \overline{\mathbf{x}}) = \frac{1}{2\mathbf{i}} \left(\overline{\mathbf{x}} - \frac{a-b}{a+b} \mathbf{x} \right), \tag{2.14}$$

while if $\mathbf{x} \in P'$, $\mathbf{z}$ lies outside the unit circle and $\mathbf{z}^\star \in \mathring{\mathcal{C}}$, so that the velocity becomes

$$\overline{\mathbf{u}}(\mathbf{x}) = \frac{1}{2\mathbf{i}} \frac{ab}{a^2 - b^2} \left(\sqrt{\mathbf{x} + c} - \sqrt{\mathbf{x} - c} \right)^2. \tag{2.15}$$

However, in the present case the splitting of the Schwarz function (2.12) can be easily performed:

$$\mathbf{\Phi}[\mathbf{z}(\mathbf{x})] = \underbrace{\frac{a-b}{a+b} \mathbf{x}}_{\mathbf{F}(\mathbf{x})} + \underbrace{ab \frac{2}{\mathbf{x} + \sqrt{\mathbf{x}^2 - c^2}}}_{\mathbf{G}(\mathbf{x})}, \tag{2.16}$$

which still gives the fields (2.14) and (2.15) through the relation (1.2). As discussed above, when the functional form of the Schwarz function is rather simple, as in (2.12), the old formulation (1.2) is convenient with respect to the new one (2.9). This is not the case of the class of vortices investigated in the present paper.

3. The Schwarz function with two pole singularities

The present paper deals with a uniform vortex having Schwarz function of its boundary with two pole singularities (it is worth noticing that the vortex having Schwarz function of its boundary with only the pole $\mathbf{z}_1$: $\mathbf{\Phi}(\mathbf{z}) = \overline{\mathbf{x}}(\mathbf{z}) = \mathbf{a}_1/(\mathbf{z} - \mathbf{z}_1)$ is a circular, with center in $\mathbf{x}(\mathbf{z}_1)$ and radius $a_1 |\mathbf{w}_1/(\mathbf{w}_1 - \mathbf{z}_1)|$) on a suitable transformed plane, with the aim to investigate the corresponding self-induced velocity field. For $\mathbf{z} \in \mathcal{C}$, the Schwarz function

$$\mathbf{\Phi}(\mathbf{z}) = \overline{\mathbf{x}}(\mathbf{z}) = \frac{\mathbf{a}_1}{\mathbf{z} - \mathbf{z}_1} + \frac{\mathbf{a}_2}{\mathbf{z} - \mathbf{z}_2} \tag{3.1}$$

is considered. The residues $\mathbf{a}_1$, $\mathbf{a}_2$ in (3.1) are assumed to be nonvanishing complex numbers (notice that one of them, e.g. $\mathbf{a}_1$, can be assumed unitary without loss of generality), while the poles $\mathbf{z}_1$, $\mathbf{z}_2$ are chosen outside $\mathcal{C}$ and the origin ($\mathbf{z}_{1,2} \neq 0$). It is also assumed that their conjugates with respect to $\mathcal{C}$, that is, $1/\overline{\mathbf{z}}_1 =: \mathbf{w}_1$ and $1/\overline{\mathbf{z}}_2 =: \mathbf{w}_2$, satisfy the two conditions $\mathbf{z}_1 \neq \mathbf{w}_2$ and $\mathbf{z}_2 \neq \mathbf{w}_1$. The Schwarz function (3.1) gives the position $\mathbf{x} \in \partial P$ in the point $\mathbf{z} \in \mathcal{C}$ as

$$\mathbf{x}(\mathbf{z}) = -\left(\overline{\mathbf{a}}_1 \mathbf{w}_1 + \overline{\mathbf{a}}_2 \mathbf{w}_2 \right) - \frac{\overline{\mathbf{a}}_1 \mathbf{w}_1^2}{\mathbf{z} - \mathbf{w}_1} - \frac{\overline{\mathbf{a}}_2 \mathbf{w}_2^2}{\mathbf{z} - \mathbf{w}_2}. \tag{3.2}$$

The point $\mathbf{x}(\mathbf{z})$ given by (3.2) can move counterclockwise or clockwise along ∂P, even if $\mathbf{z}$ runs always counterclockwise on $\mathcal{C}$. In order to specify the direction in which $\mathbf{x}(\mathbf{z})$ moves on ∂P, a parameter σ is introduced, which holds +1 when $\mathbf{x}$ runs counterclockwise and −1 in the other case. It will be evaluated in Section 4.

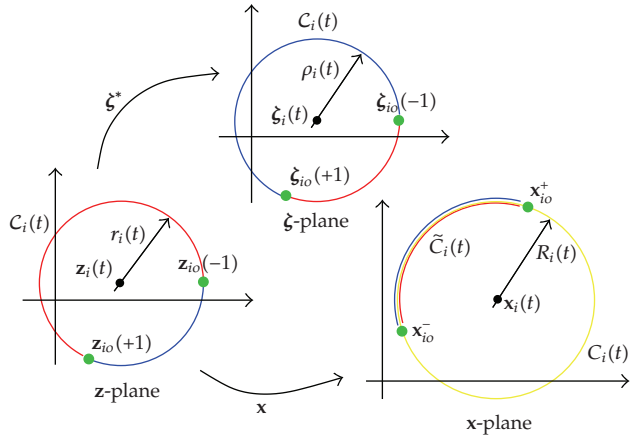

Figure 2: Sketch of the invariant circle $\mathcal{C}_i(t)$ in the planes of the variables $\mathbf{z}$ and $\boldsymbol{\zeta}$ and its image $\widetilde{C}_i(t)$ in the physical plane. The points $\mathbf{z}_{io}(\pm 1)$ and their images $\mathbf{x}_{io}^{\pm}$ are represented with green dots. The same colours (blue and red) are used for the arcs that are images through the maps $\mathbf{z} \mapsto \boldsymbol{\zeta}^\star$ and $\mathbf{z} \mapsto \mathbf{x}$ of the two arcs in which $\mathcal{C}_i(t)$ is divided by the points $\mathbf{z} = \mathbf{z}_{io}(\pm 1)$. For $\mathbf{z}$ running on $\mathcal{C}_i(t)$, the point $\mathbf{x}(\mathbf{z})$ moves on the closed curve $\widetilde{C}_i(t)$, first in a direction and then in the reverse one. $\widetilde{C}_i(t)$ is composed by two superimposed arcs of the circle $C_i(t)$ (yellow line) between the points $\mathbf{x}_{io}^-$ and $\mathbf{x}_{io}^+$: its inside has a vanishing area.

Analytic continuations of the Schwarz function (3.1) and of the map (3.2) outside $\mathcal{C}$ will be considered in the following, so that the definition of the inverse map $\mathbf{x} \mapsto \mathbf{z}$ outside the vortex boundary needs also to be discussed (see Section 6). It is shown that $\mathbf{z}(\mathbf{x})$ exists almost everywhere, unless on a closed curve $\widetilde{C}_i$, the inside of which has a vanishing area (see Figure 2).

3.1. Constants α, β, and γ

In the following, the poles and the corresponding residues of the Schwarz function (3.1) will often appear combined into the constants:

$$\boldsymbol{\alpha} = \overline{\mathbf{a}}_1 \mathbf{w}_1^2 + \overline{\mathbf{a}}_2 \mathbf{w}_2^2, \qquad \boldsymbol{\beta} = \mathbf{w}_1 \mathbf{w}_2 \left(\overline{\mathbf{a}}_1 \mathbf{w}_1 + \overline{\mathbf{a}}_2 \mathbf{w}_2\right), \qquad \boldsymbol{\gamma} = \mathbf{w}_1^2 \mathbf{w}_2^2 \left(\overline{\mathbf{a}}_1 + \overline{\mathbf{a}}_2\right); \tag{3.3}$$

moreover the related quantities: $\boldsymbol{\alpha}\overline{\boldsymbol{\beta}} = \alpha\beta \exp(\mathbf{i}\omega)$, $\boldsymbol{\beta}\overline{\boldsymbol{\gamma}} = \beta\gamma \exp(\mathbf{i}\chi)$, $\boldsymbol{\beta}' = \boldsymbol{\beta}/(\mathbf{w}_1\mathbf{w}_2)$, and $\boldsymbol{\gamma}' = \boldsymbol{\gamma}/(\mathbf{w}_1\mathbf{w}_2)$ will be also employed. In terms of the above constants, for example, the compact form of a vector $\boldsymbol{\tau}$ which is tangent to the vortex boundary on its point $\mathbf{x}(\mathbf{z})$:

$$\boldsymbol{\tau} = \mathbf{i}\mathbf{z} \frac{\boldsymbol{\alpha}\mathbf{z}^2 - 2\boldsymbol{\beta}\mathbf{z} + \boldsymbol{\gamma}}{\left(\mathbf{z} - \mathbf{w}_1\right)^2 \left(\mathbf{z} - \mathbf{w}_2\right)^2}, \tag{3.4}$$

is obtained. The function (3.4) suggests a first constraint on the Schwarz one (3.1): $\boldsymbol{\tau}$ cannot vanish on $\mathcal{C}$. The nonvanishing zeros of $\boldsymbol{\tau}$ are given by $(\boldsymbol{\beta} \pm \mathbf{i}\boldsymbol{\delta})/\boldsymbol{\alpha} =: \mathbf{z}_{io}(\pm 1)$, with $\boldsymbol{\delta}$ being the branch of the square root of $\boldsymbol{\alpha}\boldsymbol{\gamma} - \boldsymbol{\beta}^2$ for which $\overline{\boldsymbol{\beta}}\boldsymbol{\delta} + \boldsymbol{\beta}\overline{\boldsymbol{\delta}} \geq 0$ (see also Appendix D. Notice that $\boldsymbol{\delta} \neq 0$ and its modulus verifies the relation $\delta^4 = \alpha^2\gamma^2 - 2\alpha\beta^2\gamma \cos\nu + \beta^4$, with ν being the phase difference $\omega - \chi$). As a consequence, in order to enforce $\boldsymbol{\tau}(\mathbf{z}) \neq 0$ on the unit circle, the points

$\mathbf{z}_{io}(\pm 1)$ are hereafter assumed external to $\mathcal{C}$. Other important constraints will be discussed in the next section.

3.2. Map $\mathbf{z} \mapsto \boldsymbol{\zeta}^\star$ and constraints on Schwarz function

The Schwarz function (3.1) cannot be assigned in an arbitrary way: for the curve $\mathbf{x}(\mathcal{C})$ is the boundary of a uniform vortex, it must be simple. This constraint can be enforced by requiring that for any $\mathbf{z} \in \mathcal{C}$, the equation in $\boldsymbol{\zeta} : \mathbf{x}(\boldsymbol{\zeta}) = \mathbf{x}(\mathbf{z})$ has no other solutions on $\mathcal{C}$, unless $\boldsymbol{\zeta} = \mathbf{z}$. The only solution $\boldsymbol{\zeta}$ of that equation which differs from $\mathbf{z}$ is

$$\boldsymbol{\zeta} = \frac{\boldsymbol{\beta}\mathbf{z} - \boldsymbol{\gamma}}{\boldsymbol{\alpha}\mathbf{z} - \boldsymbol{\beta}} =: \boldsymbol{\zeta}^\star(\mathbf{z}), \tag{3.5}$$

so that the above condition results to be equivalent to the one: $|\boldsymbol{\zeta}^\star(\mathbf{z})| \neq 1$ for each $\mathbf{z} \in \mathcal{C}$. Equation (3.5) implies also that the points $\mathbf{z}$ and $\boldsymbol{\zeta}^\star(\mathbf{z})$ go on the same point $\mathbf{x}(\mathbf{z})$: the analytic continuation of the function (3.2) cannot be defined on the whole $\mathbf{z}$-plane, but only on a suitable subset of it including $\mathcal{C}$ (see Section 5).

It is worth noticing here that the function (3.5) maps the points $\mathbf{w}_1$ and $\mathbf{w}_2$ (on which $\mathbf{x}$ goes to the infinity) one in the other one and viceversa: for this reason these points $\mathbf{w}_1$ and $\mathbf{w}_2$ will be called hereafter as "*conjugate*" through the map $\mathbf{z} \mapsto \boldsymbol{\zeta}^\star$. Moreover, $\mathbf{z} = \infty$ goes in $\boldsymbol{\zeta}^\star = \boldsymbol{\beta}/\boldsymbol{\alpha} =: \boldsymbol{\zeta}^\star_\infty$ and viceversa $\mathbf{z} = \boldsymbol{\zeta}^\star_\infty$ is mapped in $\boldsymbol{\zeta}^\star = \infty$; the same occurs for $\mathbf{z} = 0$, which goes in $\boldsymbol{\zeta}^\star = \boldsymbol{\gamma}/\boldsymbol{\beta} =: \boldsymbol{\zeta}^\star_0$ and viceversa $\mathbf{z} = \boldsymbol{\zeta}^\star_0$ is transformed in $\boldsymbol{\zeta}^\star = 0$. More details about the map $\mathbf{z} \mapsto \boldsymbol{\zeta}^\star$ can be found in Appendix A, in particular the "viceversa" parts of the above statements are trivial consequences of the property (A.1). As well known and summarized also in that appendix, $\boldsymbol{\zeta}^\star$ transforms any circle in another circle. In the important example of the unit circle, its image $\boldsymbol{\zeta}^\star(\mathcal{C}) =: \mathcal{C}^\star$ is for $\alpha \neq \beta$, the circle having center $\boldsymbol{\zeta}_c(1)$ and radius $\rho_c(1)$ given by the following relations:

$$\boldsymbol{\zeta}_c(1) = \boldsymbol{\zeta}^\star_\infty + \frac{\beta^2}{\alpha^2 - \beta^2}\left(\boldsymbol{\zeta}^\star_\infty - \boldsymbol{\zeta}^\star_0\right), \qquad \rho_c(1) = \frac{\delta^2}{\left|\beta^2 - \alpha^2\right|}, \tag{3.6}$$

while $\mathcal{C}^\star$ becomes a straight line in the case of $\alpha = \beta$. As discussed below, the position of $\mathcal{C}^\star$ relative to $\mathcal{C}$ will be one of the key-points in order to understand the analytical structure of the velocity (see Section 4).

Coming back to the constraint on $\mathbf{x}(\mathcal{C})$, the condition $|\boldsymbol{\zeta}^\star(\mathbf{z})| = 1$ with $\mathbf{z} = \exp(\mathbf{i}\theta)$ leads from the definition (3.5) to the following equation in θ:

$$\frac{\beta^2 - 2\beta\gamma\cos(\theta + \chi) + \gamma^2}{\alpha^2 - 2\alpha\beta\cos(\theta + \omega) + \beta^2} = 1, \tag{3.7}$$

which has no solutions if and only if

$$\left|\alpha^2 - \gamma^2\right| > 2\beta R, \tag{3.8}$$

where $R^2(\alpha, \gamma \mid \nu) = |\boldsymbol{\alpha}\overline{\boldsymbol{\beta}} - \boldsymbol{\beta}\overline{\boldsymbol{\gamma}}|/\beta^2 = \alpha^2 - 2\alpha\gamma\cos\nu + \gamma^2 \geq (\alpha - \gamma)^2$. If the constraint (3.8) is verified, $\mathcal{C}^\star$ cannot intersect $\mathcal{C}$: this fundamental property, implying that ∂P is a simple curve,

depends only on the function $\boldsymbol{\zeta}^\star$ (3.5), or on the constants $\boldsymbol{\alpha}$, $\boldsymbol{\beta}$, and $\boldsymbol{\gamma}$ (3.3). Hereafter, it will be assumed always satisfied.

3.3. Invariant circles for the map $\mathbf{z} \mapsto \boldsymbol{\zeta}^\star$

An interesting issue about the map $\mathbf{z} \mapsto \boldsymbol{\zeta}^\star$ (3.5) lies in searching a circle which is transformed in itself by $\boldsymbol{\zeta}^\star$: such a circle will be called *invariant*. Two families at one parameter ($t \in \mathbb{R}$) of invariant circles have been found. In the first (and most important) one, center and radius, indicated with $\mathbf{z}_i$, r_i in the $\mathbf{z}$-plane and with $\boldsymbol{\zeta}_i$, ρ_i in the $\boldsymbol{\zeta}$-plane, are the following functions of t:

$$\mathbf{z}_i(t) \equiv \boldsymbol{\zeta}_i(t) = \boldsymbol{\zeta}^\star_\infty + \frac{\boldsymbol{\delta}}{\boldsymbol{\alpha}} t, \qquad r_i(t) \equiv \rho_i(t) = \frac{\delta}{\alpha}\sqrt{t^2+1} \tag{3.9}$$

(the branch of the square root $\boldsymbol{\delta}$ affects the sign of t, but not the definition of the center). Centers (3.9) move along a straight line parallel to $\boldsymbol{\delta}/\boldsymbol{\alpha}$ and passing on the point $\boldsymbol{\zeta}^\star_\infty$ for t running on the real axis. The importance of the circles of the first family lies in the fact that one of them (called $\mathcal{C}_i(t)$ hereafter, see Figure 2) will be used in order to define the inverse map $\mathbf{x} \mapsto \mathbf{z}$. It divides the complex plane in two parts which are mapped one in the other by the function $\boldsymbol{\zeta}^\star$ (3.5), one of them being the image of the physical plane. As shown in Figure 2, another interesting feature of $\mathcal{C}_i(t)$ is that its image $\mathbf{x}[\mathcal{C}_i(t)]$, called $\widetilde{C}_i(t)$, results from the overlapping of two equal arcs of a circle $C_i(t)$ (see Appendix E for details): for $\mathbf{z}$ running on $\mathcal{C}_i(t)$, $\mathbf{x}(\mathbf{z})$ moves along $\widetilde{C}_i(t)$ first in a direction and then in the reverse one. The branch of the inverse map, as well as the geometry of the two arcs on $C_i(t)$ (unless their endpoints, which do not change with t), will depend on the value of the parameter t (see Appendix D).

Centers of the second family lie along the straight line orthogonal to the one of the first family, but still passing through the point $\boldsymbol{\zeta}^\star_\infty$. Center and radius of a circle are in that case the functions of t:

$$\mathbf{z}_{io}(t) \equiv \boldsymbol{\zeta}_{io}(t) = \boldsymbol{\zeta}^\star_\infty + \mathbf{i}\frac{\boldsymbol{\delta}}{\boldsymbol{\alpha}} t, \qquad r_{io}(t) \equiv \rho_{io}(t) = \frac{\delta}{\alpha}\sqrt{t^2-1}, \tag{3.10}$$

$|t|$ being larger than 1. An inspection of the formulae (3.9) and (3.10) shows that circles of the first family intersect on the points $\mathbf{z}_{io}(\pm 1)$. Notice also that $\mathcal{C}_i(t)$ is divided into two complementary arcs by the points $\mathbf{z}_{io}(\pm 1)$: if the point $\mathbf{z}$ runs on $\mathcal{C}_i(t)$ from $\mathbf{z}_{io}(-1)$ to $\mathbf{z}_{io}(+1)$ in the counterclockwise sense, its image $\boldsymbol{\zeta}^\star(\mathbf{z})$ moves on the same circle and between the same points, but in the reverse direction. Finally, it is found that the function $\mathbf{z} \mapsto \mathbf{x}$ maps the points $\mathbf{z}_{io}(\pm 1)$ in the endpoints $\mathbf{x}^\pm_{io}$ of the two arcs of $C_i(t)$ which form $\widetilde{C}_i(t)$.

4. Vortex classification

A classification of the vortices having the Schwarz function of their boundaries of the form (3.1) will be proposed below. It is based on two important properties of the maps $\mathbf{z} \mapsto \boldsymbol{\zeta}^\star$ (3.5) and $\mathbf{z} \mapsto \mathbf{x}$ (3.2) and allows us to build the inverse map $\mathbf{x} \mapsto \mathbf{z}$ and then the analytical velocity field.

The first property specifies the relative position of the curve $\mathcal{C}^\star$ with respect to the unit circle (hereafter, the case $\alpha = \beta$, in which the circle $\mathcal{C}^\star$ becomes a straight line, is excluded): $\mathcal{C}^\star$ can be internal to $\mathcal{C}$ (the vortex is classified of kind 1), or external and including $\mathcal{C}$

Table 1: Behaviour with respect to the first property, consequences on the position of the circle $\mathcal{C}^\star = \boldsymbol{\zeta}^\star(\mathcal{C})$, and corresponding constraints on α, β, and γ. The quantities β_l and β_u are defined in (B.1).

Kind	Relative position of $\mathcal{C}^\star$ and $\mathcal{C}$	Constraints
1	$\mathcal{C}^\star$ internal to $\mathcal{C}$	$\alpha > \beta$, γ and $\beta < \beta_l$
2	$\mathcal{C}^\star$ includes $\mathcal{C}$	$\beta < \alpha < \gamma$
3	$\mathcal{C}^\star$ external to $\mathcal{C}$ and not including it	$\alpha < \beta < \gamma$ and $\beta < \beta_u$

Table 2: Behaviour with respect to the second property, consequences on the map $\mathbf{z} \mapsto \mathbf{x}$ and corresponding constraints on the poles $\mathbf{z}_1$, $\mathbf{z}_2$.

Kind	$\mathbf{x}(\mathscr{A})$	Position of $\mathcal{C}^\star$	Constraints on $\mathbf{z}_1$, $\mathbf{z}_2$
1	Inside P	Internal to $\mathcal{C}$	One inside and one outside $\mathcal{C}$
		External to $\mathcal{C}$	Both inside $\mathcal{C}$
2	Outside P	Internal to $\mathcal{C}$	Both outside $\mathcal{C}$
		External to $\mathcal{C}$	One inside and one outside $\mathcal{C}$

(kind 2), or external and not including $\mathcal{C}$ (kind 3). Vortices of the first kind have the inside of $\mathcal{C}$, say $\mathring{\mathcal{C}}$, naturally decomposed as $\mathring{\mathcal{C}}^\star$ joined with an annular set external to $\mathcal{C}^\star$. In order to use compact notations, this annular set or the whole $\mathring{\mathcal{C}}$ (for vortices of kind 2 or 3) will be hereafter indicated with $\mathscr{A}$. In turn, vortices of the second kind have the inside of $\mathcal{C}^\star$ naturally decomposed as $\mathscr{A}$ joined with an annular subset external to $\mathcal{C}$, that will be indicated with $\mathfrak{D}$. For vortices of kind 3, the same symbol will indicate the unbounded region external to both circles $\mathcal{C}$ and $\mathcal{C}^\star$. Appendix B is devoted to a comprehensive discussion of the first property, the results of which are summarized in Table 1. The above classification enables us to specify where $\mathscr{A}$ goes through the function $\mathbf{z} \mapsto \boldsymbol{\zeta}^\star$: it is found (see Appendix C for details) that $\mathscr{A}$ is mapped onto itself for vortices of kind 1, while it goes onto the outside or the inside of $\mathcal{C}^\star$ for vortices of kind 2 or 3, respectively.

A second property specifies where $\mathscr{A}$ goes via the other map $\mathbf{z} \mapsto \mathbf{x}$: it can go onto the inside of the vortex (which is classified of kind 1) or onto its outside (kind 2), depending on the values of the constants β, γ and on the positions of the poles $\mathbf{z}_1$ and $\mathbf{z}_2$ with respect to the unit circle. This issue is investigated by evaluating if the image of the origin in the $\mathbf{z}$-plane (which is still the origin in the physical one) lies or not inside P. To this aim, the logarithmic index $\mathcal{I}$ of the point 0 with respect to the curve ∂P

$$\begin{aligned}\mathcal{I}(0) &= \frac{1}{2\pi\mathbf{i}}\int_{\partial P}\frac{d\mathbf{x}}{\mathbf{x}-0}\\ &= -\frac{\mathbf{w}_1\mathbf{w}_2}{2\pi\mathbf{i}\boldsymbol{\beta}}\int_{\mathcal{C}} d\mathbf{z}\left[\frac{\bar{\mathbf{a}}_1\mathbf{w}_1^2}{(\mathbf{z}-\mathbf{w}_1)^2}+\frac{\bar{\mathbf{a}}_2\mathbf{w}_2^2}{(\mathbf{z}-\mathbf{w}_2)^2}\right]\frac{(\mathbf{z}-\mathbf{w}_1)(\mathbf{z}-\mathbf{w}_2)}{\mathbf{z}(\mathbf{z}-\boldsymbol{\zeta}_0^\star)}\end{aligned} \tag{4.1}$$

is considered. The residues (times $2\pi\mathbf{i}$) of the integral (4.1) on the poles 0 and $\boldsymbol{\zeta}_0^\star$ (if they lie in $\mathring{\mathcal{C}}$) hold +1, while those on $\mathbf{w}_1$ and $\mathbf{w}_2$ (if they lie in $\mathring{\mathcal{C}}$) hold −1 (notice that both pairs of points are conjugate through the map $\mathbf{z} \mapsto \boldsymbol{\zeta}^\star$). Results of the discussion of the logarithmic index (4.1) are summarized in Table 2.

In our classification, the vortices belonging to a given class are of the same kind with respect to both properties: a class is identified by the couple of numbers which indicate the

kinds with respect to the first and second properties. As an example, vortices in the class $(3,2)$ have the circle $\mathcal{C}^\star$ external and not including $\mathcal{C}$ and $\mathbf{x}(\mathcal{A})$ is the outside of the vortex.

The last issue about the map $\mathbf{z} \mapsto \mathbf{x}$ concerns the orientation of the vortex boundary, that is, the evaluation of σ. To this aim, the logarithmic index of the point $\mathbf{x}(1)$ with respect to ∂P

$$\mathcal{I}[\mathbf{x}(1)] = \frac{1}{2\pi\mathbf{i}}\oint_{\partial P}\frac{d\mathbf{x}}{\mathbf{x}-\mathbf{x}(1)} = \frac{(\mathbf{w}_1-1)(\mathbf{w}_2-1)}{2\pi\mathbf{i}(\boldsymbol{\alpha}-\boldsymbol{\beta})}\oint_{\mathcal{C}} d\mathbf{z}\frac{\boldsymbol{\alpha}\mathbf{z}^2-2\boldsymbol{\beta}\mathbf{z}+\boldsymbol{\gamma}}{(\mathbf{z}-\mathbf{w}_1)(\mathbf{z}-\mathbf{w}_2)(\mathbf{z}-1)[\mathbf{z}-\boldsymbol{\zeta}^\star(1)]} \tag{4.2}$$

has to be evaluated: it holds $+1/2$ when ∂P is oriented counterclockwise and $-1/2$ in the other case. In the last integral, the residue (multiplied times $2\pi\mathbf{i}$) on the point 1 holds $+1/2$, the ones on $\mathbf{w}_1$ and $\mathbf{w}_2$ (if they lie in $\mathring{\mathcal{C}}$) give -1 and the residue on $\boldsymbol{\zeta}^\star(1)$ (if it lies inside $\mathcal{C}$) holds $+1$. By accounting for the behaviour with respect to the second property summarized in Table 2, it can be easily shown that any vortex of kind 1 has a counterclockwise ($\sigma = +1$) oriented boundary, while the orientation of the boundary of any vortex of kind 2 is clockwise ($\sigma = -1$).

5. Geometrical discussion

In the present section, the information about the maps $\mathbf{z} \mapsto \boldsymbol{\zeta}^\star$ and $\mathbf{z} \mapsto \mathbf{x}$ given in Sections 3 and 4 are joined to give a comprehensive picture of their geometrical properties. In order to reach an intuitive representation of the behaviour of these functions, in Figures 3, 4, and 5 families of circles will be transformed through these two maps. Hence, the circles and their images are drawn with the same colour.

Our analysis starts from vortices of kind 1 with respect to the first property, having $\mathcal{C}^\star \subset \mathring{\mathcal{C}}$. For such vortices, the function $\mathbf{z} \mapsto \boldsymbol{\zeta}^\star$ maps $\mathcal{A}$ onto itself, while it goes onto $\mathring{P}$ (e.g., $\mathbf{z}_1 \in \mathring{\mathcal{C}}$, $\mathbf{z}_2$ outside, see Table 2) or onto P' ($\mathbf{z}_1$, $\mathbf{z}_2$ outside $\mathcal{C}$, see Table 2) through the map $\mathbf{z} \mapsto \mathbf{x}$. In Figure 3, samples of the planes $\mathbf{z}$ (Figures 3(a) and 3(d)), $\boldsymbol{\zeta}$ (Figures 3(b) and 3(e)), and $\mathbf{x}$ (Figures 3(c) and 3(f)) for vortices of kind $(1,1)$ (first row) and $(1,2)$ (second row) are shown.

In order to determine a branch of the inverse function $\mathbf{z}(\mathbf{x})$, a neighbourhood of $\mathcal{C}$ in the $\mathbf{z}$-plane must be defined, such that its image through the map $\mathbf{z} \mapsto \boldsymbol{\zeta}^\star$ is just its complementary set. This goal is reached by defining two subsets $\mathcal{A}_o$ and $\mathcal{A}_i$ of $\mathcal{A}$ which go one in the other one through that map: they are necessarily separated by an invariant circle of the first family $\mathcal{C}_i(t) \subset \mathcal{A}$, so that $\mathcal{A}_o$ and $\mathcal{A}_i$ lie outside and inside $\mathcal{C}_i(t)$, respectively. The value of t is chosen in the following way. As shown in Appendix D, two circles of the first family, corresponding to the values t_1 and t_2 (D.4) of the parameter, are tangent to $\mathcal{C}$ and then to $\mathcal{C}^\star$, at the same time. It follows that every invariant circle $\mathcal{C}_i(t)$ for $t_1 < t < t_2$ lies inside $\mathcal{A}$ and then is a good candidate for our aims. In Figure 3, the parameter is chosen as the mean value $(t_1+t_2)/2 =: t$. Once the subsets $\mathcal{A}_i$ and $\mathcal{A}_o$ have been introduced, by joining $\mathcal{A}_o$ with the outside of $\mathcal{C}$ a neighbourhood of the unit circle is obtained, on which the behaviour of the maps $\mathbf{z} \mapsto \boldsymbol{\zeta}^\star$ and $\mathbf{z} \mapsto \mathbf{x}$ is investigated. To this aim, in Figures 3(a) and 3(d) two sets of circles are considered, one outside $\mathcal{C}$ and the other one inside $\mathcal{A}_o$. Their images through the map $\mathbf{z} \mapsto \boldsymbol{\zeta}^\star$ are shown in Figures 3(b) and 3(e), respectively. Circles inside $\mathcal{A}_o$ go inside $\mathcal{A}_i$, while circles outside $\mathcal{C}$ are transformed in circles lying inside $\mathcal{C}^\star$. The behaviour of the map $\mathbf{z} \mapsto \mathbf{x}$ is then shown in Figures 3(c) and 3(f): in the first row, circles in $\mathcal{A}_o$ are mapped in curves lying inside the vortex, while circles outside $\mathcal{C}$ are transformed in curves external to the vortex. The contrary

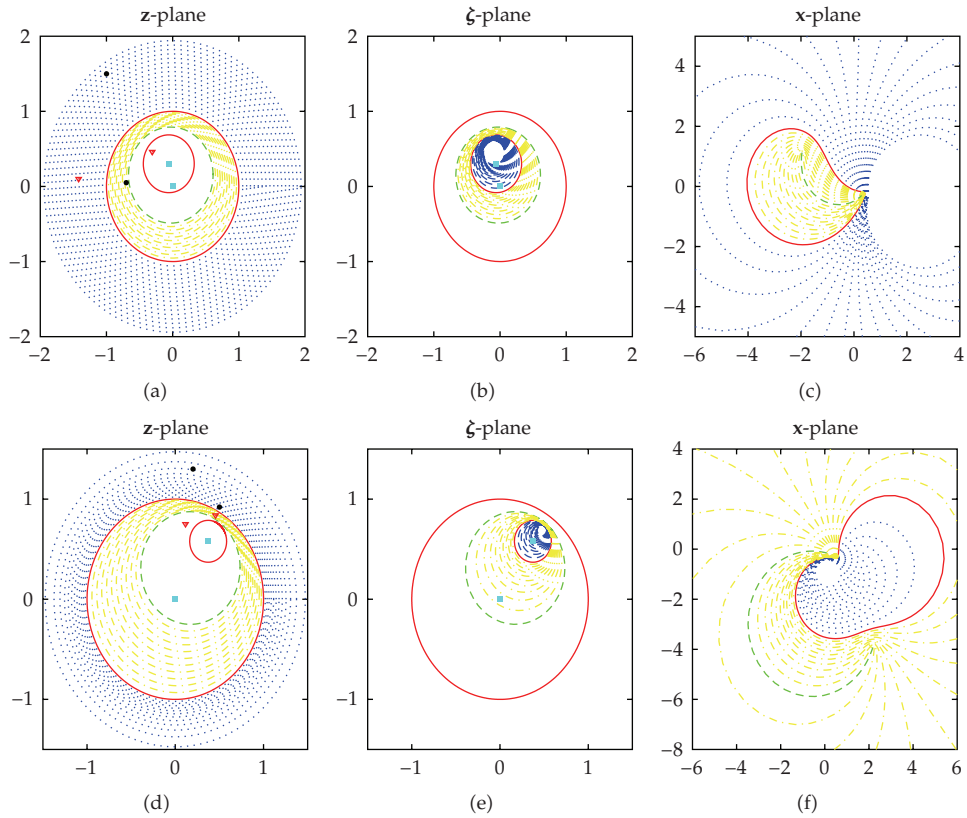

Figure 3: Planes of the variables: $\mathbf{z}$ (first column), $\boldsymbol{\zeta}$ (second), and $\mathbf{x}$ (third) for vortices of kind 1 with respect to the first property. In the first row, a vortex of kind $(1,1)$ ($\mathbf{a}_1 = 1$, $\mathbf{a}_2 = 0.1 + \mathbf{i}$, $\mathbf{z}_1 = -0.70 + 0.05\mathbf{i}$, $\mathbf{z}_2 = -1.0 + 1.5\mathbf{i}$) and in the second one a vortex of kind $(1,2)$ ($\mathbf{a}_1 = 1$, $\mathbf{a}_2 = -0.2 - 0.1\mathbf{i}$, $\mathbf{z}_1 = 0.2 + 1.3\mathbf{i}$, $\mathbf{z}_2 = 0.50 + 0.92\mathbf{i}$) are investigated. Two families of circles are considered in the $\mathbf{z}$-plane: one inside $\mathcal{A}_o$ (yellow lines) and the other one outside $\mathcal{C}$ (blue lines). Image curves (that are still circles in the $\boldsymbol{\zeta}$-plane) are drawn with the corresponding colours. Circles $\mathcal{C}$, $\mathcal{C}^\star$ (a), (b), (d), and (e) are drawn with red lines, as well as the vortex boundaries in (c) and (f). Invariant circles $\mathcal{C}_i(t)$ are drawn with green lines in (a), (b), (c), and (d). The same line is used to draw $\widetilde{\mathcal{C}}_i(t)$ in (c) and (f). The centers of $\mathcal{C}$ and $\mathcal{C}^\star$ (squared filled symbols), the poles $\mathbf{z}_1$ and $\mathbf{z}_2$ (solid black circular symbols) and the conjugate points (empty triangular symbols) $\mathbf{w}_1$ and $\mathbf{w}_2$ are also drawn.

occurs in the second row. In other words, the branch of the inverse map $\mathbf{x} \mapsto \mathbf{z}$ corresponding to the present choice of the parameter t is such that the image of $\mathring{P}$ is $\mathcal{A}_o$ (first row) or the outside of $\mathcal{C}$ (second row), while the image of P' is the outside of $\mathcal{C}$ (first row) or $\mathcal{A}_o$ (second row).

In Figure 4, the above analysis is extended to vortices of kind $(2,1)$ (first row) and $(2,2)$ (second row): as discussed below, the main difference between this case and the other ones lies in the boundness of the image of the physical plane through the inverse map $\mathbf{x} \mapsto \mathbf{z}$. Being the vortex of kind 2 with respect to the first property, the image circle $\mathcal{C}^\star = \boldsymbol{\zeta}^\star(\mathcal{C})$ includes $\mathcal{C}$. In the first row, both poles belong to $\mathring{\mathcal{C}}$ (see Table 2), so that $\mathbf{w}_1$ and $\mathbf{w}_2 \in \mathfrak{D}$, while in the second row $\mathbf{z}_1 \in \mathring{\mathcal{C}}$ and $\mathbf{z}_2$ lies outside $\mathcal{C}$ (see Table 2), so that $\mathbf{w}_2 \in \mathring{\mathcal{C}}$ and $\mathbf{w}_1$ is external to $\mathcal{C}^\star$. The set $\mathring{\mathcal{C}}$ is mapped by the function $\mathbf{z} \mapsto \boldsymbol{\zeta}^\star$ onto the outside of the image circle $\mathcal{C}^\star$, while the annular region $\mathfrak{D}$ is transformed onto itself by the same function. As above, two

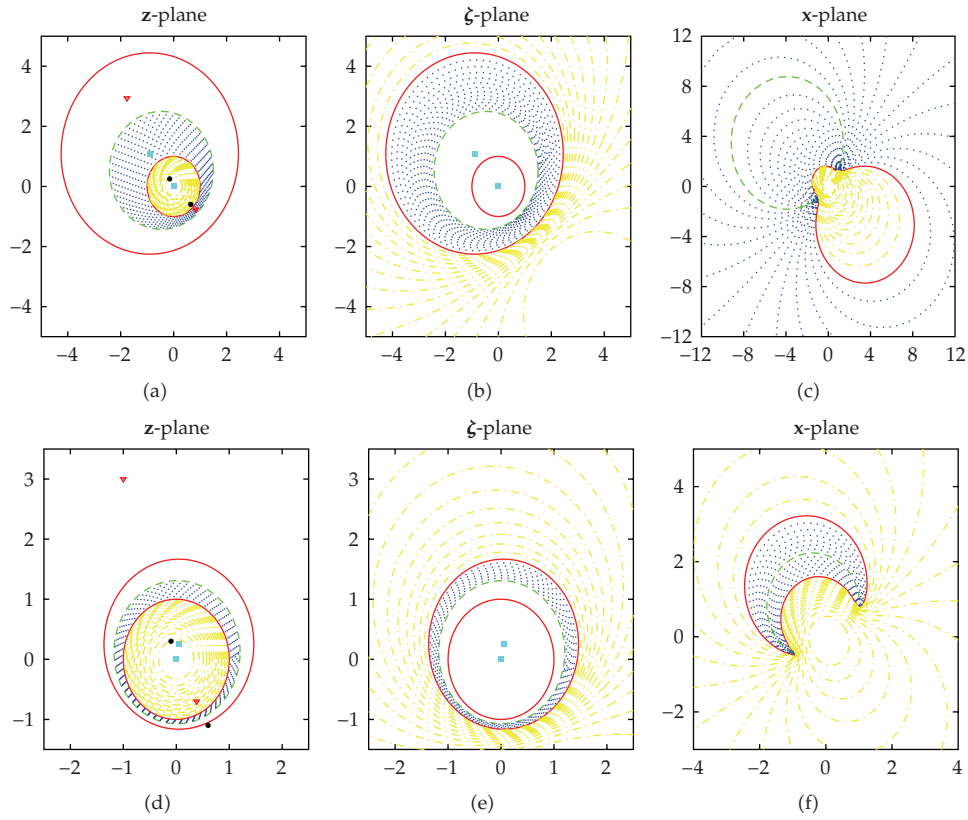

Figure 4: As in Figure 3, but for vortices of kind $(2,1)$ (first row, with $\mathbf{a}_1 = 1$, $\mathbf{a}_2 = 0.8 - 0.2\mathbf{i}$, $\mathbf{z}_1 = 0.65 - 0.60\mathbf{i}$, and $\mathbf{z}_2 = -0.15 + 0.25\mathbf{i}$) and of kind $(2,2)$ (second row, with $\mathbf{a}_1 = 1$, $\mathbf{a}_2 = 0.8 - 0.2\mathbf{i}$, $\mathbf{z}_1 = 0.6 - 1.1\mathbf{i}$, and $\mathbf{z}_2 = -0.1 + 0.3\mathbf{i}$).

complementary subsets $\mathfrak{D}_i$ and $\mathfrak{D}_o$ of $\mathfrak{D}$ (one going in the other one and viceversa through the map $\mathbf{z} \mapsto \boldsymbol{\zeta}^\star$) are identified as the parts of $\mathfrak{D}$ inside ($\mathfrak{D}_i$) or outside ($\mathfrak{D}_o$) an invariant circle of the first family belonging to $\mathfrak{D}$ (its t is still chosen as the mean value between the ones corresponding to the tangent circles). In order to explain the behaviours of the maps $\mathbf{z} \mapsto \boldsymbol{\zeta}^\star$ and $\mathbf{z} \mapsto \mathbf{x}$ (Figures 3(a) and 3(d)), two sets of circles have been considered in Figures 4(a) and 4(d): one inside $\mathcal{C}$ (yellow dashed lines) and the other one inside $\mathfrak{D}_i$ (blue). The image circles through the map $\mathbf{z} \mapsto \boldsymbol{\zeta}^\star$ are drawn in Figures 4(b) and 4(e). Finally, in Figures 4(c) and 4(f) the image curves through the function $\mathbf{z} \mapsto \mathbf{x}$ are shown: the inside of the unit circle is mapped in the inside (first row) or in the outside (second) of the vortex and $\mathfrak{D}_i$ goes onto the complementary set. A neighbourhood $\mathfrak{D}_i \cup \mathring{\mathcal{C}}$ of the curve $\mathcal{C}$ is determined, with its image through the map $\mathbf{z} \mapsto \mathbf{x}$ filling the whole physical plane.

Vortices of kind $(3,1)$ (first row) and $(3,2)$ (second row) are investigated in Figure 5: they have image circles $\mathcal{C}^\star$ external and not including $\mathcal{C}$. In Figure 5(a), the poles $\mathbf{z}_1$ and $\mathbf{z}_2$ belong to the inside of the unit circle so that $\mathbf{w}_1$ and $\mathbf{w}_2 \in \mathfrak{D}$, while in Figure 5(b) $\mathbf{z}_1 \in \mathring{\mathcal{C}}$ and $\mathbf{z}_2$ lies outside the unit circle: as a consequence, $\mathbf{w}_2 \in \mathring{\mathcal{C}}$ and $\mathbf{w}_1 \in \mathring{\mathcal{C}}^\star$. Also in the present case, $\mathfrak{D}$ is divided in two subsets $\mathfrak{D}_i$ and $\mathfrak{D}_o$ through the introduction of a suitable invariant circle: the choice of its parameter t is not obvious, but comprehensive details can be found in Appendix D. The subset $\mathfrak{D}_i$ is defined as the outside of the unit circle which lies inside $\mathcal{C}_i(t)$

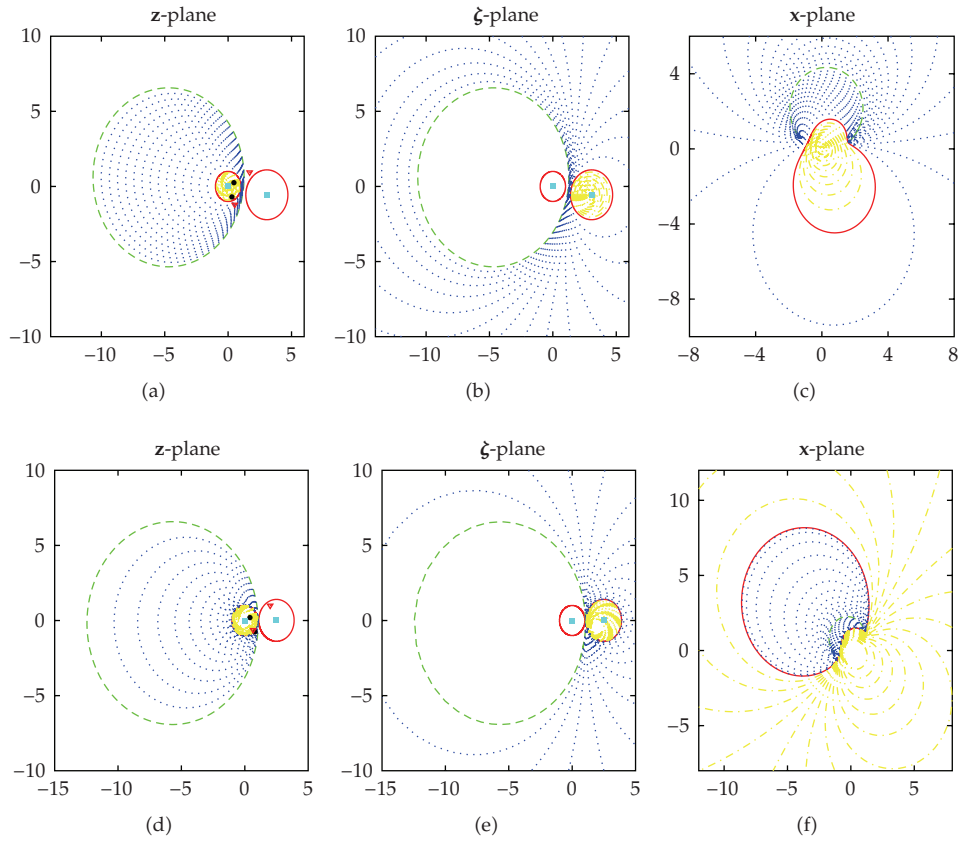

Figure 5: As in Figure 3, but for vortices of kind $(3,1)$ (first row, with $\mathbf{a}_1 = 1$, $\mathbf{a}_2 = 0.5 - 0.1\mathbf{i}$, $\mathbf{z}_1 = 0.3 - 0.7\mathbf{i}$, and $\mathbf{z}_2 = 0.45 + 0.25\mathbf{i}$) and of kind $(3,2)$ (second row, with $\mathbf{a}_1 = 1$, $\mathbf{a}_2 = 0.5 - 0.1\mathbf{i}$, $\mathbf{z}_1 = 0.80 - 0.75\mathbf{i}$, and $\mathbf{z}_2 = 0.4 + 0.2\mathbf{i}$).

(if $\mathcal{C} \subset \mathring{\mathcal{C}}_i(t)$, as in Figure 5) or outside it (if $\mathcal{C}^\star \subset \mathring{\mathcal{C}}_i(t)$). With the neighbourhood $\mathring{\mathcal{C}} \cup \mathfrak{D}_i$ of $\mathcal{C}$ being the image of the physical plane through the inverse map $\mathbf{x} \mapsto \mathbf{z}$, two sets of circles: one inside $\mathfrak{D}_i$ (blue dashed lines) and the other one in $\mathring{\mathcal{C}}$ (yellow), are introduced in order to give a picture of the behaviours of the maps $\mathbf{z} \mapsto \boldsymbol{\zeta}^\star$ (Figures 5(b) and 5(e)) and $\mathbf{z} \mapsto \mathbf{x}$ (Figures 5(c) and 5(f)). As discussed before, $\mathring{\mathcal{C}}$ goes onto $\mathring{\mathcal{C}}^\star$ and $\mathfrak{D}_i$ onto $\mathfrak{D}_o$ through the function $\mathbf{z} \mapsto \boldsymbol{\zeta}^\star$. Moreover, the function $\mathbf{z} \mapsto \mathbf{x}$ maps the inside of the unit circle onto the inside or the outside of the vortex of kind $(3,1)$ or $(3,2)$, respectively.

We are now ready to use the analysis of the maps $\mathbf{z} \mapsto \boldsymbol{\zeta}^\star$ and $\mathbf{z} \mapsto \mathbf{x}$ to obtain the analytical form of the velocity field induced by the vortex.

6. Inverse map and general form of the velocity field

In the present section, the inverse map $\mathbf{x} \mapsto \mathbf{z}$ is explicitly built and then the velocity (2.9) is analytically evaluated. Before calculating the inverse function, the following quantities:

$$\boldsymbol{\varepsilon}_1 = \mathbf{w}_1 \sqrt{\bar{\mathbf{a}}_1}, \qquad \boldsymbol{\varepsilon}_2 = \mathbf{w}_2 \sqrt{\bar{\mathbf{a}}_2}, \tag{6.1}$$

have to be introduced for the sake of simplicity of the algebraic calculations. They enable us to write the quantity $\boldsymbol{\delta}$ without square roots. Indeed, $\boldsymbol{\delta}^2 = \boldsymbol{\alpha}\boldsymbol{\gamma} - \boldsymbol{\beta}^2 = (\mathbf{w}_1 - \mathbf{w}_2)^2\boldsymbol{\varepsilon}_1^2\boldsymbol{\varepsilon}_2^2$, so that the roots (6.1) can be chosen to give $\boldsymbol{\delta} = (\mathbf{w}_1 - \mathbf{w}_2)\boldsymbol{\varepsilon}_1\boldsymbol{\varepsilon}_2$. The inverse map $\mathbf{x} \mapsto \mathbf{z}$ is then built by solving the second degree algebraic equation in $\mathbf{z} : \mathbf{x}(\mathbf{z}) = \mathbf{x}$. From the definition (3.2) of the map $\mathbf{z} \mapsto \mathbf{x}$ one obtains

$$\mathbf{z}(\mathbf{x}) = \frac{\mathbf{w}_1 + \mathbf{w}_2}{2} + \frac{(\mathbf{w}_1 - \mathbf{w}_2)(\mathbf{x} - \mathbf{x}_{io}^+)^{1/2}(\mathbf{x} - \mathbf{x}_{io}^-)^{1/2} - \boldsymbol{\alpha}}{2(\mathbf{x} + \boldsymbol{\beta}')}, \tag{6.2}$$

in which the zeros $\mathbf{x}_{io}^{\pm}$ of the discriminant have the following form:

$$\mathbf{x}_{io}^{\pm} = \frac{(\mathbf{w}_2\boldsymbol{\varepsilon}_1 \pm \mathbf{i}\mathbf{w}_1\boldsymbol{\varepsilon}_2)^2}{\mathbf{w}_1\mathbf{w}_2(\mathbf{w}_1 - \mathbf{w}_2)} = \mathbf{x}[\mathbf{z}_{io}(\pm 1)]. \tag{6.3}$$

The branches of the square roots in the inverse (6.2) must be carefully chosen through the considerations about the map $\mathbf{z} \mapsto \mathbf{x}$ that are discussed below. However, from the inverse point of view, it is only important to know if the branches are equal (i.e., both roots use $\arg(\mathbf{x} - \mathbf{x}_{io}^{\pm})/2$ or both $\arg(\mathbf{x} - \mathbf{x}_{io}^{\pm})/2 + \pi$) or different: an integer k is introduced, which holds 2 in the first case and 1 in the second one. It will be found that k changes in passing from the inside to the outside of unbounded regions as the ones in Figure 6, obtained by joining the arc of the circle C_i superimposed on $\widetilde{C}_i$ with two half straight lines parallel to the real axis and departing from the points $\mathbf{x}_{io}^{\pm}$.

The index k on a given point $\mathbf{x}$ is calculated by performing the following two steps. In the first one, the parameter t is related to the phase difference $\Delta\omega = \omega^+ - \omega^-$ between the vectors $\mathbf{x}' - \mathbf{x}_{io}^+$ and $\mathbf{x}' - \mathbf{x}_{io}^-$ for $\mathbf{x}' \in \widetilde{C}_i(t)$ (see Figure 6). This particular phase difference will be indicated with $\Delta\omega^\star$ and does not depend on the position $\mathbf{x}'$ on $\widetilde{C}_i$: as shown in Figure 6, if φ is the nonoriented and positive angle (in turn, φ can be related to t via the function $f(t)$ (E.14)) between the vectors $\mathbf{x}' - \mathbf{x}_{io}^+$ and $\mathbf{x}' - \mathbf{x}_{io}^-$ in a fixed $\mathbf{x}' \in \widetilde{C}_i$, $\Delta\omega^\star$ is identically given by $+\varphi$ in Figure 6(a) and by $-\varphi$ in Figure 6(b) for any $\mathbf{x}' \in \widetilde{C}_i$. The second step consists in relating the phase difference $\Delta\omega - \Delta\omega^\star$ in the given $\mathbf{x}$ to the corresponding value of the index k, by replacing t with the proper function of $\Delta\omega^\star$ (6.5).

The starting point is the equation

$$\left| \frac{(\boldsymbol{\varepsilon}_1 - \mathbf{i}\boldsymbol{\varepsilon}_2)(1 - \mathbf{i}t)(\mathbf{x}' - \mathbf{x}_{io}^+)^{1/2} + (\boldsymbol{\varepsilon}_1 + \mathbf{i}\boldsymbol{\varepsilon}_2)(1 + \mathbf{i}t)(\mathbf{x}' - \mathbf{x}_{io}^-)^{1/2}}{(\boldsymbol{\varepsilon}_1 - \mathbf{i}\boldsymbol{\varepsilon}_2)(\mathbf{x}' - \mathbf{x}_{io}^+)^{1/2} - (\boldsymbol{\varepsilon}_1 + \mathbf{i}\boldsymbol{\varepsilon}_2)(\mathbf{x}' - \mathbf{x}_{io}^-)^{1/2}} \right| = \sqrt{t^2 + 1}, \tag{6.4}$$

which is obtained by enforcing that $|\mathbf{z}(\mathbf{x}') - \mathbf{z}_i| = r_i$ for $\mathbf{x}' \in \widetilde{C}_i$. By introducing the arguments τ_1, τ_2 of the vectors $\boldsymbol{\varepsilon}_1 - \mathbf{i}\boldsymbol{\varepsilon}_2$, $\boldsymbol{\varepsilon}_1 + \mathbf{i}\boldsymbol{\varepsilon}_2$ and the angle $\theta^\star = \Delta\omega^\star/2 + (\tau_1 - \tau_2)$, it leads to the relation

$$t = -\cot g\theta^\star. \tag{6.5}$$

The second step consists in evaluating the index k in the given point $\mathbf{x}$. It is achieved by reconsidering the $\mathbf{z}$-planes in Figures 3, 4, 5 and the classification with respect to the first property. Indeed, the inverse map for vortices of kind 1 (or 3 with $\mathcal{C}^\star \subset \mathring{\mathcal{C}}_i$) satisfies the

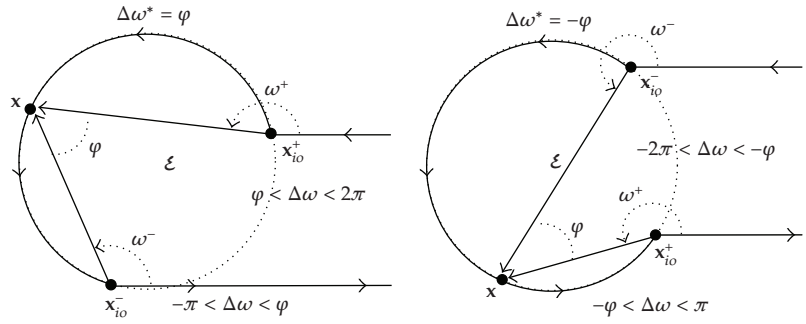

Figure 6: Qualitative behaviour of the phase difference $\Delta\omega$. Notice that if the point $\mathbf{x}^+_{io}$ moves counterclockwise on $\widetilde{C}_i(t)$ to reach $\mathbf{x}^-_{io}$, then $\Delta\omega^\star > 0$. The angle $\Delta\omega^\star$ holds identically $+\varphi$ (a) or $-\varphi$ (b) on $\widetilde{C}_i(t)$ (bold line).

Table 3: Branches to be used for the square roots $(\mathbf{x} - \mathbf{x}^+_{io})^{1/2}$ and $(\mathbf{x} - \mathbf{x}^-_{io})^{1/2}$ in any $\mathbf{x} \in \mathcal{E}$, expressed through the index k ($k = 2$ equal, $k = 1$ different). They are specified in terms of the kind of the vortex with respect to the first property (first column) and of the phase difference $\Delta\omega^\star$ (second column). Here it has been assumed that $\sin\theta^\star > 0$, while if $\sin\theta^\star < 0$, the complementary value $3 - k$ has to be considered.

Kind	Range of $\Delta\omega^\star$	k
1 or 3 with $\mathring{\mathcal{C}}_i(t) \supset \mathcal{C}^\star$	$(-2\pi, -\pi) \cup (0, +\pi)$	1
	$(-\pi, 0) \cup (+\pi, +2\pi)$	2
2 or 3 with $\mathring{\mathcal{C}}_i(t) \supset \mathcal{C}$	$(-2\pi, -\pi) \cup (0, +\pi)$	2
	$(-\pi, 0) \cup (+\pi, +2\pi)$	1

relation $|\mathbf{z}(\mathbf{x}) - \mathbf{z}_i| > r_i$. On the contrary, the same map for vortices of kind 2 (or 3 with $\mathcal{C} \subset \mathring{\mathcal{C}}_i$) verifies the opposite condition $|\mathbf{z}(\mathbf{x}) - \mathbf{z}_i| < r_i$. By introducing the function $g = \sin[(\Delta\omega - \Delta\omega^\star)/2]$, the conditions $|\mathbf{z}(\mathbf{x}) - \mathbf{z}_i| \gtrless r_i$ together with the relation (6.5) lead to the inequalities

$$(-1)^k g \lesseqgtr 0, \tag{6.6}$$

for $\sin\theta^\star > 0$, or to the opposite ones for $\sin\theta^\star < 0$. On the basis of the relations (6.6), k is defined by the sign of g, which in turn follows from the behaviour of the phase difference $\Delta\omega$ inside and outside $\mathcal{E}$. In the case of Figure 6(a), $(\Delta\omega - \Delta\omega^\star)/2$ belongs to intervals $(0, \pi - \varphi/2)$ inside and $(-\pi/2 - \varphi/2, 0)$ outside $\mathcal{E}$: the function g is positive inside and negative outside. The contrary occurs in the case of Figure 6(b): $(\Delta\omega - \Delta\omega^\star)/2$ belongs to the intervals $(-\pi + \varphi/2, 0)$ inside and $(0, \pi/2 + \varphi/2)$ outside $\mathcal{E}$: g is negative inside and positive outside. The present discussion can be extended to cover the more general case in which the half straight lines departing from $\mathbf{x}^\pm_{io}$ have other intersections with the curve $\widetilde{C}_i$. Results of such analysis are summarized in Table 3, in terms of the values of $\Delta\omega^\star$.

Once the index k has been calculated, the final issue about the inverse map $\mathbf{x} \mapsto \mathbf{z}$ (6.2) concerns it asymptotic behaviour, which can be written in the following form:

$$\mathbf{z}(\mathbf{x}) = \mathbf{w}_k - \frac{\overline{\mathbf{a}}_k \mathbf{w}_k^2}{\mathbf{x}} + O\left(\frac{1}{\mathbf{x}^2}\right), \tag{6.7}$$

with k being the index measured inside $\mathcal{E}$. For the sake of simplicity and without any loss of generality, the poles $\mathbf{z}_1$ and $\mathbf{z}_2$ and the corresponding residues $\mathbf{a}_1$ and $\mathbf{a}_2$ in the definition (3.1) of the Schwarz function are hereafter renamed in such a way that $\mathbf{z} \to \mathbf{w}_1$ for $\mathbf{x} \to \infty$.

The velocity in $\mathbf{x} \neq -\boldsymbol{\beta}'$ follows from the general form (2.9), via the change of variables from $\mathbf{y} \in \partial P$ to $\boldsymbol{\zeta} \in \mathcal{C}$:

$$\overline{\mathbf{u}}(\mathbf{x}, \overline{\mathbf{x}}) = \frac{1}{2\mathbf{i}} \left\{ \chi_P(\mathbf{x}) \overline{\mathbf{x}} + \frac{1}{2\pi\mathbf{i}} \frac{1}{\mathbf{x} + \boldsymbol{\beta}'} \int_{\mathcal{C}} d\boldsymbol{\zeta} \frac{(\boldsymbol{\alpha}\boldsymbol{\zeta}^2 - 2\boldsymbol{\beta}\boldsymbol{\zeta} + \boldsymbol{\gamma}) \boldsymbol{\Phi}(\boldsymbol{\zeta})}{(\boldsymbol{\zeta} - \mathbf{w}_1)(\boldsymbol{\zeta} - \mathbf{w}_2)[\boldsymbol{\zeta} - \mathbf{z}(\mathbf{x})][\boldsymbol{\zeta} - \mathbf{z}^\star(\mathbf{x})]} \right\}, \tag{6.8}$$

with $\mathbf{z}^\star(\mathbf{x})$ being $\boldsymbol{\zeta}^\star[\mathbf{z}(\mathbf{x})]$. Fixing a point $\mathbf{x}$ as different from $\mathbf{x}_1$ or $\mathbf{x}_2$, the velocity contribution $\overline{\mathbf{u}}[\mathbf{z}]$ of the corresponding inverse point $\mathbf{z}(\mathbf{x})$, if it lies inside $\mathcal{C}$, follows as

$$\overline{\mathbf{u}}[\mathbf{z}](\mathbf{x}) = -\frac{\sigma}{2\mathbf{i}} \boldsymbol{\Phi}[\mathbf{z}(\mathbf{x})], \tag{6.9}$$

which is evaluated by inserting the inverse value $\mathbf{z}(\mathbf{x})$ (6.2) inside the definition (3.1) of the Schwarz function $\boldsymbol{\Phi}$. On the contrary, if $\mathbf{z}^\star(\mathbf{x})$ lies inside $\mathcal{C}$, an analogous contribution is produced with $\mathbf{z}^\star$ replacing $\mathbf{z}$. Moreover, the velocity contribution of a pole $\mathbf{z}_m$ ($m = 1, 2$), if it lies inside $\mathcal{C}$, has the form of a point vortex/source singularity:

$$\begin{aligned} \overline{\mathbf{u}}[\mathbf{z}_m](\mathbf{x}) &= \frac{\sigma \mathbf{a}_m}{2\mathbf{i}} \left\{ \frac{1}{\mathbf{z} - \mathbf{z}_m} + \frac{1}{(\mathbf{z}_m - \mathbf{w}_1)(\mathbf{z}_m - \mathbf{w}_2)} \left[(\mathbf{z}_m - \mathbf{z}_m^\star) - \frac{(\mathbf{z}_m^\star - \mathbf{w}_1)(\mathbf{z}_m^\star - \mathbf{w}_2)}{\mathbf{z} - \mathbf{z}_m^\star} \right] \right\} \\ &= \frac{\Gamma_m + \mathbf{i}\mu_m}{2\pi\mathbf{i}} \frac{1}{\mathbf{x} - \mathbf{x}_m}, \end{aligned} \tag{6.10}$$

where the (complex) intensity of the point vortex/source is

$$\Gamma_m + \mathbf{i}\mu_m = \sigma\pi \mathbf{a}_m \left[\overline{\mathbf{a}}_1 \left(\frac{\mathbf{w}_1}{\mathbf{z}_m - \mathbf{w}_1} \right)^2 + \overline{\mathbf{a}}_2 \left(\frac{\mathbf{w}_2}{\mathbf{z}_m - \mathbf{w}_2} \right)^2 \right]. \tag{6.11}$$

On the point $\mathbf{x}_m$ ($m = 1, 2$), that is, $\mathbf{z} \to \mathbf{z}_m$ or $\mathbf{z} \to \mathbf{z}_m^\star$, the pole $\mathbf{z}_m$ becomes of multiplicity two. In both cases, the contribution to the velocity ($m' = 3 - m$) is as follows:

$$\overline{\mathbf{u}}[\mathbf{z}_m](\mathbf{x}_m) = \overline{\mathbf{u}}[\mathbf{z}_m^\star](\mathbf{x}_m) = \frac{\sigma}{2\mathbf{i}} \left[\mathbf{a}_m \left(\frac{1}{\mathbf{z}_m - \mathbf{w}_1} + \frac{1}{\mathbf{z}_m - \mathbf{w}_2} - \frac{1}{\mathbf{z}_m - \mathbf{z}_m^\star} \right) - \frac{\mathbf{a}_{m'}}{\mathbf{z}_m - \mathbf{z}_{m'}} \right]. \tag{6.12}$$

Finally, the contribution of the point $\mathbf{w}_m$ ($m = 1, 2$), if it lies inside $\mathcal{C}$, is constant:

$$\overline{\mathbf{u}}[\mathbf{w}_m](\mathbf{x}) \equiv \frac{\sigma}{2\mathbf{i}} \boldsymbol{\Phi}(\mathbf{w}_m). \tag{6.13}$$

On the point $\mathbf{x} = -\boldsymbol{\beta}'$, which corresponds to $\mathbf{z} \to \infty$ and $\mathbf{z}^\star = \boldsymbol{\beta}/\boldsymbol{\alpha}$, the following form of the velocity is obtained:

$$\overline{\mathbf{u}}(-\boldsymbol{\beta}') = \frac{1}{2\mathbf{i}}\left[\chi_P(\mathbf{x})\overline{\mathbf{x}} + \frac{1}{2\pi\mathbf{i}}\frac{1}{\boldsymbol{\alpha}}\int_{\mathcal{C}} d\boldsymbol{\zeta}\frac{(\boldsymbol{\alpha}\boldsymbol{\zeta}^2 - 2\boldsymbol{\beta}\boldsymbol{\zeta} + \boldsymbol{\gamma})\boldsymbol{\Phi}(\boldsymbol{\zeta})}{(\boldsymbol{\zeta} - \mathbf{w}_1)(\boldsymbol{\zeta} - \mathbf{w}_2)(\boldsymbol{\zeta} - \boldsymbol{\zeta}^\star_\infty)}\right]. \tag{6.14}$$

Also in this case the contribution of a pole $\mathbf{w}_m$ $(m = 1, 2)$ assumes the previous form (6.13), while the one of the pole $\boldsymbol{\zeta}^\star_\infty$ is $-\sigma\boldsymbol{\Phi}(\boldsymbol{\zeta}^\star_\infty)/(2\mathbf{i})$, according to the formula (6.9) in $\mathbf{z}^\star(\mathbf{x})$. In the next section, the velocity is explicitly built for each kind of vortices and comparisons with suitable simple vortices are carried out in order to explain the dependence of velocity and streamfunction on the vortex shape.

7. Analysis of the velocity field

In the present section, the velocity and streamfunction fields for the six classes of vortices introduced before (see in particular Section 5) are built, by accounting for the different contributions evaluated in the previous section and the orientation of the vortex boundary established in Section 4. All the fields, with the only exception of the external velocity field for the vortices of kind $(2,1)$, involve the inverse map $\mathbf{x} \mapsto \mathbf{z}$ which has been analyzed in the previous section. It is also found that vortices of kinds $(3,1)$, $(3,2)$ have the same analytical structure of the velocity of the ones of kinds $(2,1)$, $(2,2)$, respectively.

7.1. Vortices of kind $(1,1)$

Our analysis starts from vortices of kind $(1,1)$, which have the pole $\mathbf{z}_1$ inside $\mathcal{C}$, while $\mathbf{z}_2$ lies outside: as a consequence $\mathbf{w}_1$ lies outside $\mathcal{C}$ and $\mathbf{w}_2$ inside $\mathcal{C}^\star$. The velocity in a point $\mathbf{x}$ of the physical plane is the following one:

$$\overline{\mathbf{u}}(\mathbf{x}) = \frac{\chi_P(\mathbf{x})}{2\mathbf{i}}\left\{\overline{\mathbf{x}} - \boldsymbol{\Phi}\left[\mathbf{z}(\mathbf{x})\right]\right\} - \frac{1}{2\mathbf{i}}\left\{\boldsymbol{\Phi}\left[\mathbf{z}^\star(\mathbf{x})\right] - \boldsymbol{\Phi}\left(\mathbf{w}_2\right)\right\} + \frac{\Gamma_1 + \mathbf{i}\mu_1}{2\pi\mathbf{i}}\frac{1}{\mathbf{x} - \mathbf{x}_1}, \tag{7.1}$$

the behaviour of which in neighbourhoods of the point $\mathbf{x}_1$, of the closed curves ∂P and $\widetilde{C}_i(t)$, as well as at infinity must be discussed. First of all, it is worth noticing that the field is regular in a neighbourhood of $\mathbf{x}_1$: the singular behaviour of $1/(\mathbf{x} - \mathbf{x}_1)$ for $\mathbf{x} \to \mathbf{x}_1$ is corrected by $\boldsymbol{\Phi}[\mathbf{z}(\mathbf{x})]$ when $\mathbf{z}_1 \in \mathcal{A}_o$ $(\mathbf{x}_1 \in \mathring{P})$, or by $\boldsymbol{\Phi}[\mathbf{z}^\star(\mathbf{x})]$ when $\mathbf{z}_1 \in \mathcal{A}_i$ $(\mathbf{x}_1 \in \mathring{P})$ or $\mathbf{z}_1 \in \mathring{\mathcal{C}}^\star$ ($\mathbf{x}_1$ external to the vortex); see (6.10). The continuity across the vortex boundary is enforced by the definition of the Schwarz function: it implies that $\chi_P(\mathbf{x})\ \{\overline{\mathbf{x}} - \boldsymbol{\Phi}[\mathbf{z}(\mathbf{x})]\} \to 0$ for $\mathbf{x}$ going to any point on ∂P from the inside of the vortex, while that term vanishes outside P, due to the presence of the characteristic function of the vortex $\chi_P(\mathbf{x})$.

Another issue concerns the continuity of the velocity (7.1) across the closed curve $\widetilde{C}_i(t)$, which lies entirely inside the vortex in the present case. Indeed, the Schwarz function $\boldsymbol{\Phi}$ evaluated in $\mathbf{z}(\mathbf{x})$ or in $\mathbf{z}^\star(\mathbf{x})$ gives rise to a composite function of $\mathbf{x}$ which is discontinuous across that curve, due to an analogous behaviour of the inverse function $\mathbf{z}(\mathbf{x})$. As discussed in Sections 3 and 6, a point $\mathbf{x}_0$ on $\widetilde{C}_i(t)$ (different from the endpoints $\mathbf{x}^\star_1$ and $\mathbf{x}^\star_2$) must be considered as the superimposition of two points (say $\mathbf{x}'_0$ and $\mathbf{x}''_0$) which come through the map $\mathbf{z} \mapsto \mathbf{x}$ from a point $\mathbf{z}'_0 \in C_i(t)$ and from its image $\boldsymbol{\zeta}^\star(\mathbf{z}'_0) = \mathbf{z}''_0$. With these points on

$\mathcal{C}_i(t)$ being different, the limit value of $\mathbf{z}(\mathbf{x})$ in a point $\mathbf{x}_0 \in \widetilde{C}_i(t)$ from one side of that curve ($\mathbf{x} \to \mathbf{x}_0'$) or from the other side ($\mathbf{x} \to \mathbf{x}_0''$) is also different. The continuity of the velocity (7.1) is proved by noticing that the sum of the Schwarz functions calculated on both points $\mathbf{z}(\mathbf{x})$ ($\mathbf{z}_0'$ in the above discussion) and $\mathbf{z}^\star(\mathbf{x})$ (that is ($\mathbf{z}_0''$)) is in fact present into the velocity for any $\mathbf{x} \in \mathring{P}$ and that sum results to be continuous across $\widetilde{C}_i(t)$.

Finally, the field (7.1) has the right behaviour at infinity. Indeed, the inverse function $\mathbf{z}(\mathbf{x})$ goes to $\mathbf{w}_1$ (and then $\mathbf{z}^\star(\mathbf{x}) \to \mathbf{w}_2$) when $\mathbf{x} \to \infty$, as a consequence:

$$\mathbf{\Phi}\big[\mathbf{z}^\star(\mathbf{x})\big] - \mathbf{\Phi}(\mathbf{w}_2) = \frac{\mathbf{b}_{12} + b_{22}}{\mathbf{x}} + O\left(\frac{1}{\mathbf{x}^2}\right), \tag{7.2}$$

where the coefficients $\mathbf{b}_{pq} := \mathbf{a}_p \overline{\mathbf{a}}_q \mathbf{w}_q^2 / (\mathbf{z}_p - \mathbf{w}_q)^2$ for $p, q = 1, 2$ have been introduced (notice that $\mathbf{b}_{11}$ and $\mathbf{b}_{22}$ are real and positive, so that $\mathbf{b}_{11} = b_{11}$ and $\mathbf{b}_{22} = b_{22}$, moreover $\mathbf{b}_{12} = \overline{\mathbf{b}}_{21}$). By inserting the above asymptotic expansion inside the one for the velocity (7.1), one obtains

$$\overline{\mathbf{u}}(\mathbf{x}) = \frac{b_{11} - b_{22}}{2\mathbf{i}\mathbf{x}} + O\left(\frac{1}{\mathbf{x}^2}\right), \tag{7.3}$$

in which it is worth noticing that the area of the vortex is given in the present case by the following relation:

$$|P| = \frac{1}{2} \operatorname{Im}\left(\int_P d\mathbf{x}\, \mathbf{\Phi}\right) = \pi(b_{11} - b_{22}). \tag{7.4}$$

Once the above value of the area is accounted for, the asymptotic expansion (7.3) becomes the expected one: $\overline{\mathbf{u}}(\mathbf{x}) \sim |P| / (2\pi\mathbf{i}\mathbf{x})$.

On the basis of the velocity (7.1), the streamfunction which behaves as $-|P|G(\mathbf{x})$ for $\mathbf{x} \to \infty$ is now evaluated. To this aim, the velocity is rewritten in the following form:

$$\begin{aligned}
&\overline{\mathbf{u}}(\mathbf{x}) - \frac{\chi_P(\mathbf{x})}{2\mathbf{i}}\overline{\mathbf{x}} \\
&\quad = \frac{1}{2\mathbf{i}}\left[\left(\frac{\mathbf{a}_1}{\mathbf{z}_1 - \mathbf{w}_1} - \frac{\mathbf{a}_2}{\mathbf{z}_2 - \mathbf{w}_2} + \frac{\mathbf{a}_2}{\mathbf{z}_2 - \boldsymbol{\zeta}_\infty^\star}\right) + \frac{\mathbf{a}_1 \chi_{P'}(\mathbf{x})}{\mathbf{z}(\mathbf{x}) - \mathbf{z}_1} - \frac{\mathbf{a}_2 \chi_P(\mathbf{x})}{\mathbf{z}(\mathbf{x}) - \mathbf{z}_2} - \frac{\boldsymbol{\delta}^2}{\boldsymbol{\alpha}^2} \frac{\mathbf{a}_2}{\big(\mathbf{z}_2 - \boldsymbol{\zeta}_\infty^\star\big)^2} \frac{1}{\mathbf{z}(\mathbf{x}) - \mathbf{z}_2^\star}\right]
\end{aligned} \tag{7.5}$$

in which only the inverse function $\mathbf{z}(\mathbf{x})$ appears. Notice that the right-hand side of the above equation is an analytic function of $\mathbf{z}$ in its domain of definition (being $\mathbf{z} = \mathbf{z}(\mathbf{x})$, it is an analytic function of $\mathbf{x}$, too) called $\overline{\mathbf{v}}(\mathbf{z})$ hereafter. As a consequence, a complex potential $\mathbf{P}[\mathbf{z}(\mathbf{x})]$ (the imaginary part of which is just the streamfunction ψ) exists and is defined by the differential relation

$$\overline{\mathbf{v}} = \frac{d\mathbf{P}}{d\mathbf{x}} = \frac{\mathbf{P}'}{\mathbf{x}'}, \tag{7.6}$$

in which apices indicate derivatives in $\mathbf{z}$. In this way, the complex potential is calculated via an integration of the equation $\mathbf{P}' = \mathbf{x}'\overline{\mathbf{v}}$, which gives in any point $\mathbf{x}$ external to the vortex (dependences on $\mathbf{x}$ are omitted, for the sake of simplicity) the streamfunction:

$$\begin{aligned}\psi = {} & \frac{|P|}{2\pi}\log\left|\mathbf{z}-\mathbf{w}_1\right| - \frac{b_{11}}{2}\log\left|\mathbf{z}-\mathbf{z}_1\right| + \frac{b_{22}}{2}\log\left|\mathbf{z}-\mathbf{z}_2^{\star}\right| \\ & + \frac{1}{2}\mathrm{Re}\left\{\mathbf{b}_{12}\log\frac{\mathbf{z}-\mathbf{w}_2}{\mathbf{z}-\mathbf{z}_1} - \mathbf{b}_{21}\log\frac{\mathbf{z}-\mathbf{w}_2}{\mathbf{z}-\mathbf{z}_2^{\star}} + \left[\boldsymbol{\Phi}(\mathbf{w}_2)-\boldsymbol{\Phi}(\mathbf{w}_1)\right]\frac{\overline{\mathbf{a}}_2\mathbf{w}_2^2}{\mathbf{z}-\mathbf{w}_2}\right\}.\end{aligned} \tag{7.7}$$

The points $\mathbf{z}_1$, $\mathbf{z}_2^{\star}$, and $\mathbf{w}_2$ lie inside the unit circle, so that the branches which are discontinuous on the segments joining $\mathbf{z}_1$ with $\mathbf{w}_2$ and $\mathbf{w}_2$ with $\mathbf{z}_2^{\star}$ must be chosen for the first and the second complex logarithms, respectively. Moreover, by taking into account the asymptotic expansion of the inverse function $\mathbf{z}(\mathbf{x})$ (6.7), one can observe that the modulus $|\mathbf{z}-\mathbf{w}_1|$ behaves as $1/x$ for growing x: as a consequence, ψ (7.7) has the right behaviour, that is, $-|P|G(\mathbf{x})$, for $\mathbf{x}$ going to the infinity. In any point $\mathbf{x}$ belonging to the vortex the streamfunction has the form

$$\psi = -\frac{x^2}{4} - \frac{b_{22}}{2}\log\frac{\left|\mathbf{z}-\mathbf{w}_1\right|\left|\mathbf{z}-\mathbf{w}_2\right|}{\left|\mathbf{z}-\mathbf{z}_2\right|\left|\mathbf{z}-\mathbf{z}_2^{\star}\right|} + \frac{1}{2}\mathrm{Re}\left[\mathbf{b}_{21}\log\frac{(\mathbf{z}-\mathbf{z}_2)(\mathbf{z}-\mathbf{z}_2^{\star})}{(\mathbf{z}-\mathbf{w}_1)(\mathbf{z}-\mathbf{w}_2)} + \boldsymbol{\Phi}(\mathbf{w}_1)\mathbf{x}\right] + \text{const.}, \tag{7.8}$$

with the constant being evaluated by calculating in a point of the vortex boundary the external streamfunction (7.7). In (7.8), the points $\mathbf{z}_2$, $\mathbf{w}_1$ are external to $\mathcal{C}$, while the ones $\mathbf{w}_2$, $\mathbf{z}_2^{\star}$ are internal to $\mathcal{C}^{\star}$. This fact enables us to adopt the branch which is discontinuous on the straight segment joining $\mathbf{w}_2$ with $\mathbf{z}_2^{\star}$ for the logarithm $\log[(\mathbf{z}-\mathbf{w}_2)/(\mathbf{z}-\mathbf{z}_2^{\star}]$, while the branch to be used for $\log[(\mathbf{z}-\mathbf{w}_1)/(\mathbf{z}-\mathbf{z}_2)]$ depends on the positions of the points $\mathbf{w}_1$, $\mathbf{z}_2$ with respect to $\mathcal{C}$: if the segment joining $\mathbf{w}_1$ with $\mathbf{z}_2$ intersects $\mathcal{C}$, the branch which is continuous on that segment is used. On the contrary, the branch which is discontinuous on the same segment must be employed.

The streamlines for the vortex of kind $(1,1)$ in Figure 3(c) are drawn in Figure 7(a). From that figure, it appears rather hard to investigate the dependence of ψ (and then of $\mathbf{u}$) on the shape of the vortex, mainly for the presence of the prevailing isotropic component of such field, responsible for the isotropic behaviour $\psi \sim -|P|/(2\pi)\log x$ at infinity. In order to overcome this intrinsic difficulty, a Rankine vortex of unitary vorticity with center on the center of vorticity of P and area $|P|$ is considered: the induced streamfunction and velocity are indicated with ψ_R and $\mathbf{u}_R$, respectively. In Figures 7(b) and 7(c), the circular boundary of such an *equivalent* vortex P_R is drawn with green dashed lines. Now, the differences $\psi - \psi_R =: \tilde{\psi}$, $\mathbf{u}-\mathbf{u}_R =: \tilde{\mathbf{u}}$ are much more meaningful than the fields ψ, $\mathbf{u}$, with the dependence on the vortex shape of such quantities being easily identified, due to the linear behaviour with respect to the vorticity of Biot-Savàrt's law. The streamfunction $\tilde{\psi}$, as well as the differential velocity $\tilde{\mathbf{u}}$, can be interpreted as generated by a vortex having only two levels of vorticity: +1 in the parts of P that are external to Rankine's vortex ($P_R' \cap P$) and -1 in the regions of the equivalent vortex outside P ($P' \cap P_R$), while it vanishes in the central region of the vortex ($P_R \cap P$) and outside P. For the present vortex, the isolines of $\tilde{\psi}$ as well as the vectors $\tilde{\mathbf{u}}$ on a finite set of points (Figures 7(b) and 7(c)) exhibit a four-lobed structure of both fields, more evident in the streamfunction rather than in the velocity. Two intense regions are located near the tip of

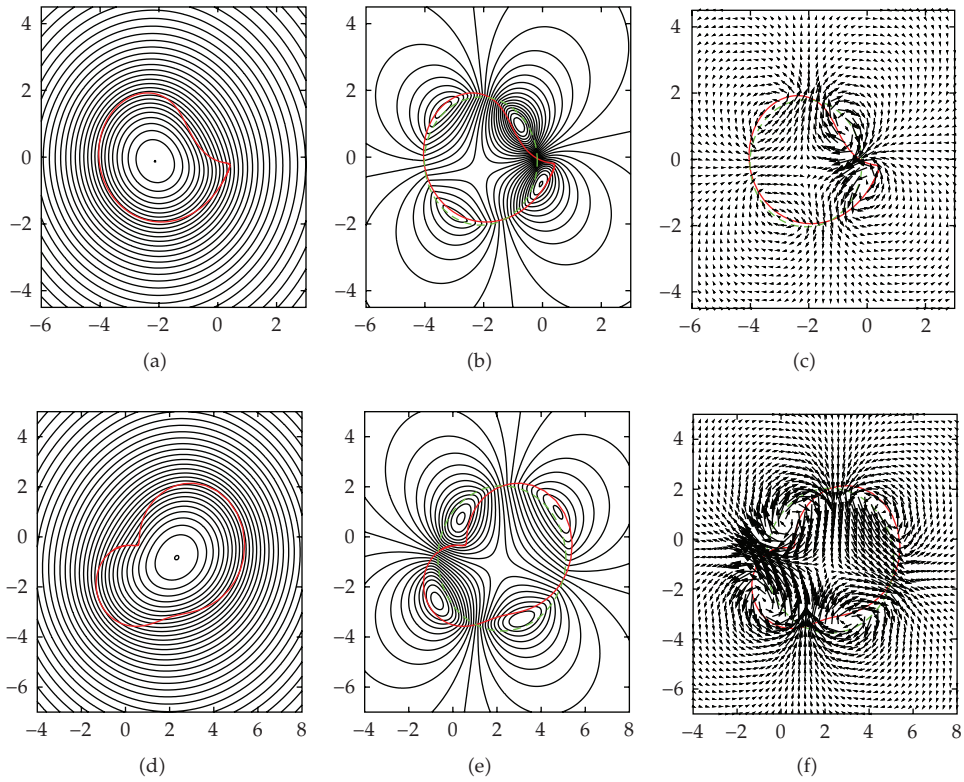

Figure 7: (a), (d) The streamlines (blue lines, (a) $\Delta\psi = 0.1$ and (d) 0.2) are drawn for the vortices in Figures 3(c) and 3(f), respectively. (b), (c), (e), (f) The boundaries of the vortices are drawn with thick red lines, while the ones of the equivalent Rankine vortices with green dashed lines. The differential streamlines and velocities (with a scale factor of 3) are shown in (b) ($\Delta\psi = 0.01$), (e) (0.04), and (c), (f), respectively.

the vortex, generated by two adjacent zones having opposite signs of the vorticity. As a result, strong ingoing velocities are produced near the tip. From Figure 7(c), it can be also seen that the velocity $\tilde{\mathbf{u}}$ vanishes in a rapid way at infinity ($\tilde{\mathbf{u}} \sim 1/x^2$ for $\mathbf{x} \to \infty$).

The above kinematical analysis enables us to investigate the onset of the filamentation of the vortex boundary in the region near the tip. According to Pullin [16], the filamentation consists in the ejection of thin streams of vorticity which "may form patterns of ever increasing complexity and apparently ever decreasing minimum spatial scale as they are convected and strained by the irrotational flow outside the vortex." A heuristic explanation of the filamentation is based on the presence in a neighbourhood of the vortex boundary of hyperbolic critical points of the velocity which "rapidly distort the vorticity and convect filaments away from the vortex core." In the present case, the evaluation of the relative streamfunction in a corotating frame, obtained by using the diagnostic ellipse approach [17] and the analytical form of the streamfunction (7.7), (7.8) shows the presence of one hyperbolic critical point near the tip: as a consequence, the vortex has high probabilities to develop filaments in that region. Even if different paths to filamentation have been proposed, the analysis of the time behaviour of the Schwarz function in a neighbourhood of the tip could offer other interesting interpretations.

7.2. *Vortices of kind* (1, 2)

A vortex of kind (1, 2) has both poles ($\mathbf{z}_1$ and $\mathbf{z}_2$) in the Schwarz function (3.1) outside $\mathcal{C}$, so that $\mathbf{w}_1 \in \mathcal{A}_o$ and $\mathbf{w}_2 \in \mathcal{A}_i$. The velocity is evaluated as

$$\overline{\mathbf{u}}(\mathbf{x}) = \frac{\chi_P(\mathbf{x})}{2\mathbf{i}}\overline{\mathbf{x}} + \frac{\chi_{P'}(\mathbf{x})}{2\mathbf{i}}\boldsymbol{\Phi}\big[\mathbf{z}(\mathbf{x})\big] - \frac{\boldsymbol{\Phi}(\mathbf{w}_1)}{2\mathbf{i}} + \frac{1}{2\mathbf{i}}\big\{\boldsymbol{\Phi}\big[\mathbf{z}^\star(\mathbf{x})\big] - \boldsymbol{\Phi}(\mathbf{w}_2)\big\}, \tag{7.9}$$

the behaviour of which in neighbourhoods of the curves ∂P and $\widetilde{C}_i(t)$, as well as at infinity, must be investigated. The velocity (7.9) is continuous across ∂P due to the definition of the Schwarz function of that curve $\boldsymbol{\Phi}$. Indeed, if $\mathbf{x} \to \mathbf{x}_0 \in \partial P$ from the inside of the vortex, the sum of the first two terms (the other ones are continuous across ∂P) gives $\overline{\mathbf{x}}_0/(2\mathbf{i})$ and the same limit value is obtained from the outside. By accounting for the property $\chi_P(\mathbf{x}_0) = \chi_{P'}(\mathbf{x}_0) = 1/2$, the above limit agrees also with the value assumed by the sum on the point $\mathbf{x}_0 \in \partial P$. About the continuity across $\widetilde{C}_i(t)$, the same explanation which has been given for the vortices of kind (1, 1) holds also in the present case, with the only difference that $\widetilde{C}_i(t)$ lies outside the vortex. The behaviour for $\mathbf{x} \to \infty$ is evaluated by considering that $\mathbf{z}(\mathbf{x}) \to \mathbf{w}_1$ and $\mathbf{z}^\star(\mathbf{x}) \to \mathbf{w}_2$ and by using the asymptotic expansion:

$$\boldsymbol{\Phi}\big[\mathbf{z}(\mathbf{x})\big] - \boldsymbol{\Phi}(\mathbf{w}_1) = \frac{b_{11} + \mathbf{b}_{21}}{\mathbf{x}} + O\left(\frac{1}{\mathbf{x}^2}\right), \tag{7.10}$$

together with the above one (7.2). It follows that $\overline{\mathbf{u}}(\mathbf{x}) \sim v|P|/(2\pi\mathbf{i}\mathbf{x})$, with the area $|P|$ of the vortex assuming in the present case the form

$$|P| = -\frac{1}{2}\,\mathrm{Im}\left(\int_P d\mathbf{x}\,\boldsymbol{\Phi}\right) = \pi\big(b_{11} + \mathbf{b}_{12} + \mathbf{b}_{21} + b_{22}\big), \tag{7.11}$$

once the clockwise orientation of the vortex boundary has been accounted for.

The streamfunction in any point $\mathbf{x}$ outside the vortex follows from the velocity field (7.9) as

$$\begin{aligned}\psi = {} & \frac{|P|}{2\pi}\log\big(|\mathbf{z}-\mathbf{w}_1||\mathbf{z}-\mathbf{w}_2|\big) - \frac{b_{11}}{2}\log\big(|\mathbf{z}-\mathbf{z}_1||\mathbf{z}-\mathbf{z}_1^\star|\big) - \frac{b_{22}}{2}\log\big(|\mathbf{z}-\mathbf{z}_2||\mathbf{z}-\mathbf{z}_2^\star|\big) \\ & - \frac{\mathbf{b}_{12}+\mathbf{b}_{21}}{4}\log\big(|\mathbf{z}-\mathbf{z}_1||\mathbf{z}-\mathbf{z}_2||\mathbf{z}-\mathbf{z}_1^\star||\mathbf{z}-\mathbf{z}_2^\star|\big) + \frac{1}{4}\mathrm{Re}\left[(\mathbf{b}_{21}-\mathbf{b}_{12})\log\frac{(\mathbf{z}-\mathbf{z}_1)(\mathbf{z}-\mathbf{z}_1^\star)}{(\mathbf{z}-\mathbf{z}_2)(\mathbf{z}-\mathbf{z}_2^\star)}\right],\end{aligned} \tag{7.12}$$

where the branches of two complex logarithms must be chosen. The first one is $\log[(\mathbf{z}-\mathbf{z}_1^\star)/(\mathbf{z}-\mathbf{z}_2^\star)]$: it is evaluated by using the branch which is discontinuous on the segment joining the point $\mathbf{z}_1^\star$ with $\mathbf{z}_2^\star$, lying that segment in $\mathring{\mathcal{C}}^\star$. In order to evaluate the second logarithm, that is $\log[(\mathbf{z}-\mathbf{z}_1)/(\mathbf{z}-\mathbf{z}_2)]$, two cases must be distinguished: if the segment joining the point $\mathbf{z}_1$ with $\mathbf{z}_2$ intersects the unit circle, the branch which is continuous on that segment must be used

and viceversa, if the above segment does not intersect $\mathcal{C}$, the branch which is discontinuous on the same segment must be adopted. The streamfunction in a point $\mathbf{x} \in \mathring{P}$ is

$$\begin{aligned}\psi = &-\frac{x^2}{4} + \frac{b_{11}}{2}\log\frac{|\mathbf{z}-\mathbf{w}_2|}{|\mathbf{z}-\mathbf{z}_1^\star|} + \frac{b_{22}}{2}\log\frac{|\mathbf{z}-\mathbf{w}_1|}{|\mathbf{z}-\mathbf{z}_2^\star|} + \frac{\mathbf{b}_{12}+\mathbf{b}_{21}}{4}\log\frac{|\mathbf{z}-\mathbf{w}_1||\mathbf{z}-\mathbf{w}_2|}{|\mathbf{z}-\mathbf{z}_1^\star||\mathbf{z}-\mathbf{z}_2^\star|} \\ &-\frac{1}{2}\mathrm{Re}\left[\frac{\bar{\mathbf{a}}_1\mathbf{w}_1^2\boldsymbol{\Phi}(\mathbf{w}_1)}{\mathbf{z}-\mathbf{w}_1} + \frac{\bar{\mathbf{a}}_2\mathbf{w}_2^2\boldsymbol{\Phi}(\mathbf{w}_2)}{\mathbf{z}-\mathbf{w}_2} + \frac{\mathbf{b}_{12}-\mathbf{b}_{21}}{2}\log\frac{(\mathbf{z}-\mathbf{z}_1^\star)(\mathbf{z}-\mathbf{w}_2)}{(\mathbf{z}-\mathbf{z}_2^\star)(\mathbf{z}-\mathbf{w}_1)}\right] + \text{const.},\end{aligned} \tag{7.13}$$

in which the above constant is calculated by evaluating (7.12) in a point $\mathbf{z} \in \mathcal{C}$. The complex logarithm is evaluated by considering that the points $\mathbf{z}_1^\star$, $\mathbf{z}_2^\star$ are internal to $\mathcal{C}^\star$, while $\mathbf{w}_1 \in \mathcal{A}_o$ and, as a consequence, $\mathbf{w}_2 \in \mathcal{A}_i$. It follows that the branches of the above logarithms to be used are discontinuous along the segments joining $\mathbf{z}_1^\star$ with $\mathbf{z}_2^\star$ and joining $\mathbf{w}_1$ with $\mathbf{w}_2$.

The isolines of the streamfunction (7.12), (7.13) for the vortex of Figure 3(f) are drawn in Figure 7(d), together with the boundary of the vortex itself (red thick line). A certain anisotropy of such field appears from the figure, but in order to quantify such behaviour it is more convenient to analyze the differential streamfunction $\tilde{\varphi}$, and the isolines are drawn in Figure 7(e). Four regions in which the differential vorticity holds +1 or −1 can be identified, while it vanishes in the region $P_R \cap P$ and outside P. As a consequence, two regions of the vortex boundary experience intense inward velocities, while in other two regions act strong outward velocities (see Figure 7(f)).

7.3. Vortices of kind $(2,1)$

Vortices of kind $(2,1)$ have both poles inside $\mathcal{C}$: as a consequence, $\mathbf{w}_1 \in \mathfrak{D}_i$ and $\mathbf{w}_2 \in \mathfrak{D}_o$. The velocity is given by

$$\overline{\mathbf{u}}(\mathbf{x}) = \frac{\chi_P(\mathbf{x})}{2\mathbf{i}}\left\{\overline{\mathbf{x}} - \boldsymbol{\Phi}\left[\mathbf{z}(\mathbf{x})\right]\right\} + \frac{1}{2\pi\mathbf{i}}\sum_{m=1}^{2}\frac{\Gamma_m + \mathbf{i}\mu_m}{\mathbf{x}-\mathbf{x}_m}, \tag{7.14}$$

in which the singularities in the points $\mathbf{x}_1$ and $\mathbf{x}_2$ are only apparent, due to the form (6.10) of the term $(\Gamma_m + \mathbf{i}\mu_m)/(\mathbf{x}-\mathbf{x}_m)$. About the form of the field (7.14) outside the vortex it is worth observing that it coincides with the one due to a couple of vortices/sources placed on the points $\mathbf{x}_1$ and $\mathbf{x}_2$. With the area $|P|$ of the vortex being given by (7.11), the relation $\Gamma_1 + \Gamma_2 + \mathbf{i}(\mu_1 + \mu_2) = |P|$ follows: the total source intensity $\mu_1 + \mu_2$ vanishes (due to the incompressible nature of the fluid).

The streamfunction in any point $\mathbf{x}$ external to the vortex has the form

$$\begin{aligned}\psi = &\frac{|P|}{2\pi}\log\left(|\mathbf{z}-\mathbf{w}_1||\mathbf{z}-\mathbf{w}_2|\right) - \frac{b_{11}}{2}\log\left(|\mathbf{z}-\mathbf{z}_1||\mathbf{z}-\mathbf{z}_1^\star|\right) - \frac{b_{22}}{2}\log\left(|\mathbf{z}-\mathbf{z}_2||\mathbf{z}-\mathbf{z}_2^\star|\right) \\ &-\frac{\mathbf{b}_{12}+\mathbf{b}_{21}}{4}\log\left(|\mathbf{z}-\mathbf{z}_1||\mathbf{z}-\mathbf{z}_2||\mathbf{z}-\mathbf{z}_1^\star||\mathbf{z}-\mathbf{z}_2^\star|\right) + \frac{1}{4}\mathrm{Re}\left[(\mathbf{b}_{21}-\mathbf{b}_{12})\log\frac{(\mathbf{z}-\mathbf{z}_1)(\mathbf{z}-\mathbf{z}_1^\star)}{(\mathbf{z}-\mathbf{z}_2)(\mathbf{z}-\mathbf{z}_2^\star)}\right].\end{aligned} \tag{7.15}$$

The first complex logarithm, that is, $\log[(\mathbf{z}-\mathbf{z}_1)/(\mathbf{z}-\mathbf{z}_2)]$, is evaluated by using the branch which is discontinuous on the segment joining $\mathbf{z}_1$ with $\mathbf{z}_2$ (internal to the unit circle), while

for the second logarithm, that is, $\log[(\mathbf{z}-\mathbf{z}_1^\star)/(\mathbf{z}-\mathbf{z}_2^\star)]$, the branch is chosen by considering the relative positions of the points $\mathbf{z}_1^\star$, $\mathbf{z}_2^\star$ with respect to the invariant circle $\mathcal{C}_i(t)$. For example, if the segment joining the point $\mathbf{z}_1^\star$ with $\mathbf{z}_2^\star$ intersects $\mathcal{C}_i(t)$, the branch which is continuous on that segment must be used. Inside the vortex the streamfunction holds:

$$\begin{aligned}\psi = &-\frac{x^2}{4} + \frac{b_{11}}{2}\log\frac{|\mathbf{z}-\mathbf{w}_2|}{|\mathbf{z}-\mathbf{z}_1^\star|} + \frac{b_{22}}{2}\log\frac{|\mathbf{z}-\mathbf{w}_1|}{|\mathbf{z}-\mathbf{z}_2^\star|} + \frac{\mathbf{b}_{12}+\mathbf{b}_{21}}{4}\log\frac{|\mathbf{z}-\mathbf{w}_1||\mathbf{z}-\mathbf{w}_2|}{|\mathbf{z}-\mathbf{z}_1^\star||\mathbf{z}-\mathbf{z}_2^\star|} \\ &+ \frac{1}{4}\mathrm{Re}\left[(\mathbf{b}_{12}-\mathbf{b}_{21})\log\frac{(\mathbf{z}-\mathbf{w}_1)(\mathbf{z}-\mathbf{z}_2^\star)}{(\mathbf{z}-\mathbf{w}_2)(\mathbf{z}-\mathbf{z}_1^\star)}\right] - \frac{1}{2}\mathrm{Re}\left[\frac{\overline{\mathbf{a}}_1\mathbf{w}_1^2\boldsymbol{\Phi}(\mathbf{w}_1)}{\mathbf{z}-\mathbf{w}_1} + \frac{\overline{\mathbf{a}}_2\mathbf{w}_2^2\boldsymbol{\Phi}(\mathbf{w}_2)}{\mathbf{z}-\mathbf{w}_2}\right] + \text{const.},\end{aligned} \tag{7.16}$$

where the constant is evaluated as above. The complex logarithms $\log[(\mathbf{z}-\mathbf{w}_1)/(\mathbf{z}-\mathbf{w}_2)]$ and $\log[(\mathbf{z}-\mathbf{z}_1^\star)/(\mathbf{z}-\mathbf{z}_2^\star)]$ are evaluated by using suitable branches which depend on the relative positions of the points $\mathbf{w}_1$, $\mathbf{w}_2$ and $\mathbf{z}_1^\star$, $\mathbf{z}_2^\star$ with respect to the unit circle. For example, if the segment joining $\mathbf{w}_1$ with $\mathbf{w}_2$ intersects $\mathcal{C}$, the branch which is continuous on that segment is used.

The isolines of the streamfunction (7.15), (7.16) are drawn in Figure 8(a): they exhibit a high level of isotropy, at least qualitatively. This is due to the small amount of circulation with respect to the total one which characterizes the vortex tip and it still suggests the analysis of the above differential fields. Indeed, the differential streamfunction $\widetilde{\psi}$, the isolines of which being drawn in Figure 8(b), enables a more quantitative analysis: an intense region generated by a differential vorticity level +1 appears in correspondence with the tip on the vortex boundary, while other regions are much less intense and then they can be discarded in a first analysis. As a consequence, intense outward and inward velocities appear before and after the tip (see Figure 8(c)), while the remaining vortex boundary appears to be quasistationary.

7.4. Vortices of kind (2, 2)

Vortices of kind (2, 2) have $\mathbf{z}_1$ external to the unit circle and $\mathbf{z}_2 \in \mathring{\mathcal{C}}$, as a consequence $\mathbf{w}_1 \in \mathring{\mathcal{C}}$ and $\mathbf{w}_2$ lies outside the image circle $\mathcal{C}^\star$. The velocity assumes the following form:

$$\overline{\mathbf{u}}(\mathbf{x}) = \frac{\chi_P(\mathbf{x})}{2\mathbf{i}}\overline{\mathbf{x}} + \frac{\chi_{P'}(\mathbf{x})}{2\mathbf{i}}\boldsymbol{\Phi}[\mathbf{z}(\mathbf{x})] - \frac{\boldsymbol{\Phi}(\mathbf{w}_1)}{2\mathbf{i}} + \frac{\Gamma_2 + \mathbf{i}\mu_2}{2\pi\mathbf{i}}\frac{1}{\mathbf{x}-\mathbf{x}_2}. \tag{7.17}$$

the behaviour of which in neighbourhoods of the point $\mathbf{x}_2$ and of the vortex boundary ∂P needs to be discussed. The apparent singularity $\mathbf{x}_2$ lies outside the vortex and, as before, it is compensated by the term $\boldsymbol{\Phi}[\mathbf{z}(\mathbf{x})]$. Moreover, if $\mathbf{x} \to \mathbf{x}_0 \in \partial P$ from the inside of the vortex, the sum of the first two terms goes to $\overline{\mathbf{x}}_0/(2\mathbf{i})$, while if $\mathbf{x} \to \mathbf{x}_0$ from the outside, the term with the Schwarz function goes to the same limit and the first one vanishes. That limit agrees also with the value of the sum on the vortex boundary due to the property of the characteristic functions: $\chi_P(\mathbf{x}_0) = \chi_{P'}(\mathbf{x}_0) = 1/2$ for $\mathbf{x}_0 \in \partial P$. The behaviour of the velocity (7.17) at infinity is the right one: $\overline{\mathbf{u}}(\mathbf{x}) \sim |P|/(2\pi\mathbf{i}\mathbf{x})$ and it follows from the asymptotic expansion (7.10) of $\boldsymbol{\Phi}[\mathbf{z}(\mathbf{x})]$, by accounting for that the area of the vortex is still given by (7.4).

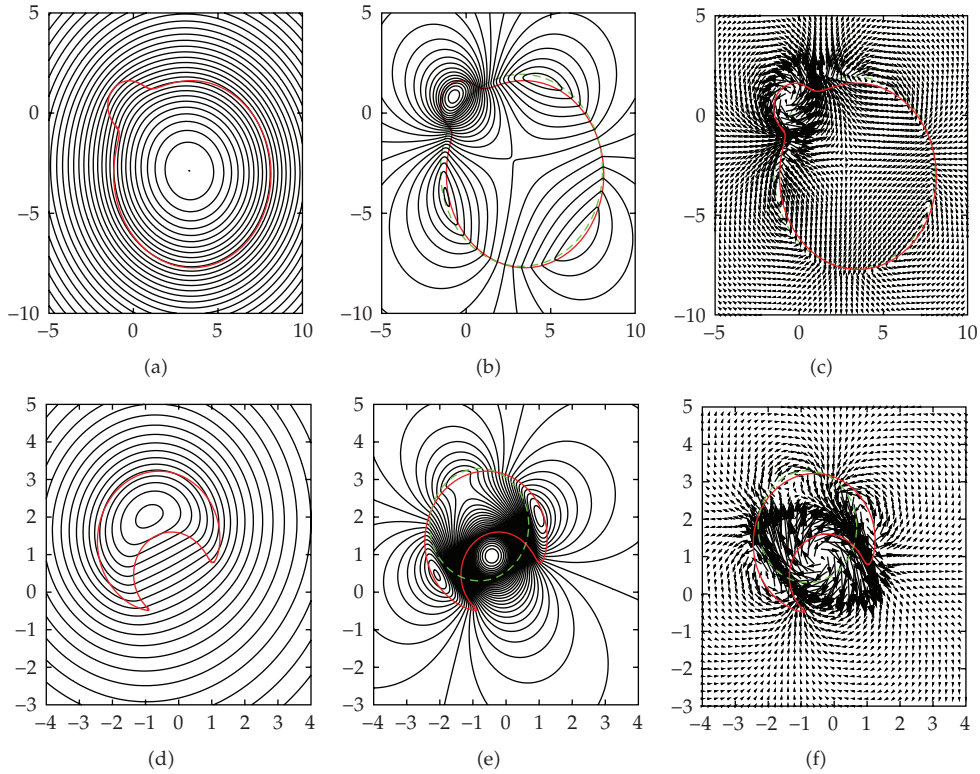

Figure 8: As in Figure 7, but for the vortices of Figures 4(c) and 4(f). The steps between two streamlines are (a) 0.5, (c) 0.1, and (b), (d) 0.04, while the scale factor in drawing the differential velocities $\tilde{\mathbf{u}}$ is 4.

The streamfunction in any point $\mathbf{x}$ external to the vortex is given by

$$\begin{aligned}\psi = {} & \frac{|P|}{2\pi}\log|\mathbf{z}-\mathbf{w}_1| - \frac{b_{11}}{2}\log|\mathbf{z}-\mathbf{z}_1| + \frac{b_{22}}{2}\log|\mathbf{z}-\mathbf{z}_2^\star| \\ & + \frac{1}{2}\mathrm{Re}\left[\mathbf{b}_{21}\log\frac{\mathbf{z}-\mathbf{z}_2^\star}{\mathbf{z}-\mathbf{w}_2} + \mathbf{b}_{12}\log\frac{\mathbf{z}-\mathbf{w}_2}{\mathbf{z}-\mathbf{z}_1} + \frac{\bar{\mathbf{a}}_2\mathbf{w}_2^2\left[\boldsymbol{\Phi}(\mathbf{w}_2)-\boldsymbol{\Phi}(\mathbf{w}_1)\right]}{\mathbf{z}-\mathbf{w}_2}\right].\end{aligned} \tag{7.18}$$

The branches used for the complex logarithms $\log[(\mathbf{z}-\mathbf{z}_2^\star)/(\mathbf{z}-\mathbf{w}_2)]$ and $\log[(\mathbf{z}-\mathbf{w}_2)/(\mathbf{z}-\mathbf{z}_1)]$ depend on the positions of the points $\mathbf{z}_2^\star$, $\mathbf{w}_2$ and $\mathbf{w}_2$, $\mathbf{z}_1$ with respect to the unit circle. For example, if the straight segment joining $\mathbf{z}_2^\star$ with $\mathbf{w}_2$ intersects $\mathcal{C}$, then the branch which is continuous on that segment is used. In any point $\mathbf{x} \in \mathring{P}$ the streamfunction is given by the following formula:

$$\psi = -\frac{x^2}{4} + \frac{b_{22}}{2}\log\frac{|\mathbf{z}-\mathbf{z}_2||\mathbf{z}-\mathbf{z}_2^\star|}{|\mathbf{z}-\mathbf{w}_1||\mathbf{z}-\mathbf{w}_2|} + \frac{1}{2}\mathrm{Re}\left[\mathbf{b}_{21}\log\frac{(\mathbf{z}-\mathbf{z}_2)(\mathbf{z}-\mathbf{z}_2^\star)}{(\mathbf{z}-\mathbf{w}_1)(\mathbf{z}-\mathbf{w}_2)} + \boldsymbol{\Phi}(\mathbf{w}_1)\mathbf{x}\right] + \text{const.}, \tag{7.19}$$

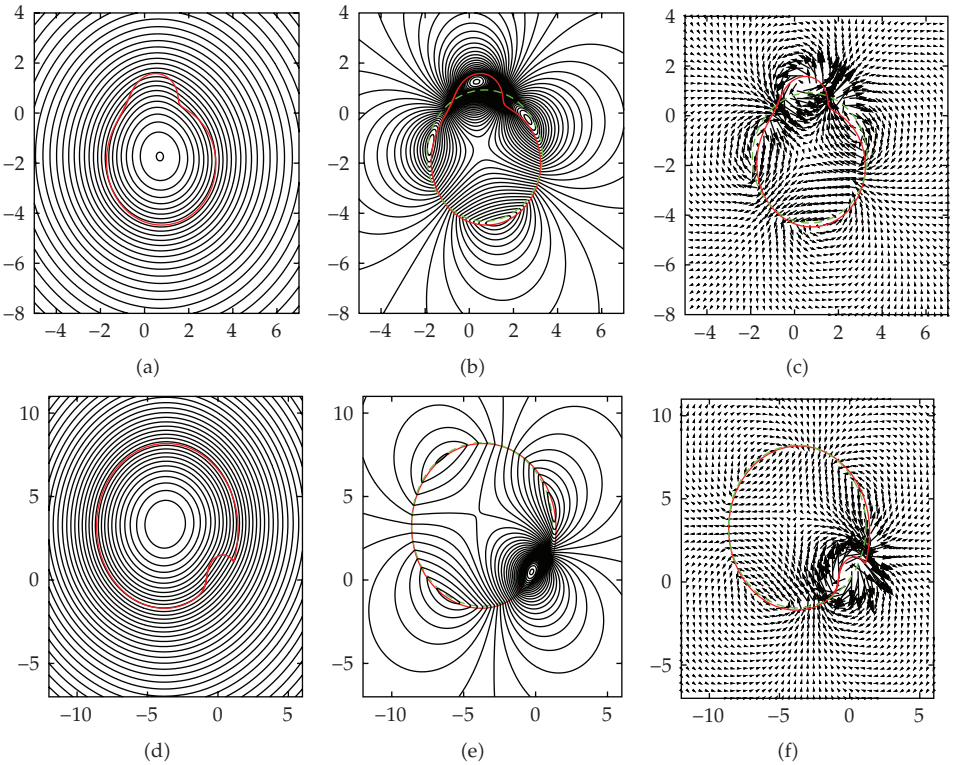

Figure 9: As in Figure 7, but for the vortices in Figures 5(c) and 5(f). The jumps between two consecutive streamlines are (a) 0.2, (b) 0.01, (d) 0.5, and (e) 0.02. The scale factors in drawing the differential velocities are (c) 5 and (f) 8.

with the constant being evaluated as described before. The first complex logarithm, that is, $\log[[\mathbf{z}-\mathbf{z}_2)/(\mathbf{z}-\mathbf{w}_1)]$, is calculated by using the branch which is discontinuous along the segment joining $\mathbf{z}_2$ with $\mathbf{w}_1$ (internal to the unit circle), while the branch employed for the second logarithm, that is, $\log[(\mathbf{z}-\mathbf{z}_2^\star)/(\mathbf{z}-\mathbf{w}_2)]$, depends on the positions of the points $\mathbf{z}_2^\star$, $\mathbf{w}_2$ with respect to the invariant circle $\mathcal{C}_i(t)$.

The isolines of the streamfunction (7.18), (7.19) are drawn in Figure 8(d): a certain anisotropy appears that becomes strongly evident in the differential streamlines of Figure 8(e). Also in this case a four-lobed structure of the field appears with a very intense region generated by a negative level of vorticity -1 near the center of vorticity. The central region is predominant on the other ones: indeed, if this picture is reread in velocity (Figure 8(f)), a strong differential clockwise velocity is found near the center of vorticity. Two less intense regions generated by counterclockwise differential vorticity are identified on both tips, leading to a very complicated distribution of normal velocities on the vortex boundary. The analysis of a relative streamfunction in a suitable rotating frame shows the presence of two hyperbolic critical points near both tips of the vortex, just outside the vortex. As it is shown by Figure 8(f), the normal differential velocities are oriented inward on the left tip and outward on the right one, so that filamentation could occur in the region near the right tip only.

7.5. Vortices of kinds (3,1) *and* (3,2)

Vortices of kind (3,1) have both poles $\mathbf{z}_1$ and $\mathbf{z}_2$ inside $\mathcal{C}$, so that $\mathbf{w}_1 \in \mathfrak{D}_i$ and $\mathbf{w}_2 \in \mathfrak{D}_o$. The velocity assumes a form identical to the one of (7.14), which holds for vortices of kind (2,1). Finally, for vortices of kind (3,2) the pole $\mathbf{z}_1$ lies outside $\mathcal{C}$, while $\mathbf{z}_2$ is internal to the same curve. As a consequence $\mathbf{w}_1 \in \mathring{\mathcal{C}}$ and $\mathbf{w}_2 \in \mathring{\mathcal{C}}^\star$ and the form assumed by the velocity is identical to the one of (7.17) which holds for vortices of kind (2,2).

The streamfunction induced by the vortex in Figure 5(c) is shown in Figure 9(a), where its isolines are drawn, together with the vortex boundary (red thick line). The streamfunction appears to be quasi-isotropic, due to the small amount of circulation, with respect to the circulation of the vortex itself, which is contained into the vortex tip. This suggest to investigate the differential streamfunction, the isolines of which are drawn in Figure 9(b), together with the boundaries of the vortex (red thick line) and of the equivalent Rankine vortex (green dashed line). From that figure, the role of the tip is clarified: it induces an intense differential streamfunction and corresponding counterclockwise velocities (see Figure 9(c)), while two regions before and after the tip are characterized by clockwise velocities. As a consequence, strong outward and inward normal velocities are experienced by the vortex boundary before and after the tip.

The streamfunction for the sample of vortex of kind (3,2) which is shown in Figure 5(f) is investigated in Figure 9(d). The isolines are quasi-isotropic, while the ones of the differential streamfunction $\widetilde{\varphi}$ (see Figure 9(e)) exhibit a strong region near the vortex tip, which generate intense clockwise velocities (Figure 9(f)). As a consequence, strong inward normal velocities appear before the tip, while outward velocities are generated just on the tip. The other part of the vortex boundary appears to be quasistationary, unless small tangential velocities in counterclockwise direction on the right and on the left of the tip, while clockwise velocities are experienced by the region of the boundary which is opposite to the tip.

8. Concluding remarks and perspectives

The present paper consists in a first application of the relation (2.9) to the study of the dependence of the self-induced velocity on the shape of the vortex. Although this shape is described in terms of only three complex parameters ($\mathbf{a}_2/\mathbf{a}_1$, $\mathbf{z}_1$ and $\mathbf{z}_2$), the corresponding family of vortices appears to be very rich and of great interest. In particular, vortices of shapes very far from the circular one can be obtained, the self-induced streamfunction and velocity of which being analytically calculated, without any approximation.

A classification of all the vortices having the Schwarz function with two simple poles is proposed, by stressing the different ways in which the inverse map $\mathbf{x} \mapsto \mathbf{z}$ is built and their consequences on the self-induced streamfunction and velocity fields. Six kinds of vortices have been identified, on the basis of the relative positions of the circles $\mathcal{C}$ and $\mathcal{C}^\star$ and of the global behaviour of the map $\mathbf{z} \mapsto \mathbf{x}$. The velocity in a point $\mathbf{x}$ is found to be a linear combination of Schwarz functions evaluated in $\mathbf{z}(\mathbf{x})$ and in $\boldsymbol{\zeta}^\star[\mathbf{z}(\mathbf{x})]$ and of pointwise source/vortex singularities, together with the contribution of the solid body rotation $\overline{\mathbf{x}}$ inside the vortex. Depending on the kind of the vortex, as well as on the fact that $\mathbf{x}$ lies inside or outside the vortex, one or more of the above terms disappear. Vortices having only Schwarz function contributes are found (kind (1,2), see Section 7.2), as well as vortices the external velocity of which is due only to two pointwise source/vortex singularities (kind (2,1), see Section 7.3). Tools to build inverse map $\mathbf{x} \mapsto \mathbf{x}$, streamfunction, and velocity for the vortices here analyzed are available on the website http://www.meccanicadeifluidi.it/. Numerical

tools (using the contour dynamics approach) for a comparison with the present analytical results may be also found.

The qualitative understanding of the analytical streamlines and velocities is strongly simplified by introducing the differential fields $\tilde{\varphi}$, $\tilde{\mathbf{u}}$ which assume the equivalent Rankine vortex P_R as the reference one. These fields are viewed as induced by the regions $P'_R \cap P$ and $P' \cap P_R$, where the vorticity holds +1 and −1, respectively. The remaining part of the plane does not contribute. In a lot of vortices, a qualitative inspection to the differential fields enables us to estimate normal velocities on the vortex boundaries, which is the first step to understand their small-time dynamics.

As briefly discussed in Section 1, the final aim of such an analysis lies in representing the vortex motion by following the time evolution of the corresponding Schwarz function. At the present time, the forms (7.1), (7.9), (7.14), and (7.17) of the velocity have been used in the right-hand side of (1.4), which becomes a sum of rational functions of $\mathbf{z}$. Several important issues can be now addressed. First of all, does a vortex among the ones here analyzed that retains in time the structure of its Schwarz function exist? In other words, does the left-hand side of (1.4) have the same algebraic structure of the right one? If this is the case, the evolution equations for poles and residues can be easily deduced. Moreover, why the two sides have different poles? Were new singularities born at the initial time? and so on. In the opinion of the authors, some of the above questions could find their answers in the near future.

Appendices

A. Some properties of the map $\mathbf{z} \mapsto \boldsymbol{\zeta}^\star$

The function (3.5), known in literature as Möbius map, plays a crucial role in the present analysis. Fixing an arbitrary point $\mathbf{x}_0$ in the physical plane, this point maps the corresponding inverse point $\mathbf{z} = \mathbf{z}(\mathbf{x}_0)$ in a new one, that is $\boldsymbol{\zeta} = \boldsymbol{\zeta}^\star[\mathbf{z}(\mathbf{x}_0)]$, on which the function $\mathbf{z} \mapsto \mathbf{x}$ (3.2) still assumes the value $\mathbf{x}_0$.

The most important property is that the inverse of the map $\boldsymbol{\zeta}^\star(\mathbf{z})$ coincides with the map itself:

$$\boldsymbol{\zeta}^\star\left[\boldsymbol{\zeta}^\star(\mathbf{z})\right] \equiv \mathbf{z}, \tag{A.1}$$

so that the function $\boldsymbol{\zeta}^\star(\mathbf{z})$ is a self-inverse one. A picture of the global behaviour of the map $\boldsymbol{\zeta}^\star(\mathbf{z})$ is obtained by rewriting it in the more general form:

$$\boldsymbol{\zeta}^\star(\mathbf{z}) = \mathbf{a} + \frac{\mathbf{b}}{\mathbf{z} - \mathbf{c}} \tag{A.2}$$

(here $\mathbf{a} = \mathbf{c} = \boldsymbol{\beta}/\boldsymbol{\alpha}$ and $\mathbf{b} = (\boldsymbol{\beta}^2 - \boldsymbol{\alpha}\boldsymbol{\gamma})/\boldsymbol{\alpha}^2 \neq 0$). As it is well known, the form (A.2) is relevant, showing that $\boldsymbol{\zeta}^\star$ maps a circle $\mathcal{C}(r_c \mid \mathbf{z}_c)$ of radius r_c and center on $\mathbf{z}_c$ in another circle when the function (A.2) remains bounded, that is, $\mathbf{c}$ does not belong on $\mathcal{C}(r_c \mid \mathbf{z}_c)$.

First of all, it is proved that a redefinition of the coefficients $\mathbf{b}$ and $\mathbf{c}$ enables us to reduce the mapping of any circle to the one of the unit circle $\mathcal{C}$. Indeed, consider the circle having center on the point $\mathbf{z}_c$ and radius r_c, a point $\mathbf{z}$ of which is written as $\mathbf{z} = \mathbf{z}_c + r_c\mathbf{z}'$ for $\mathbf{z}' \in \mathcal{C}$. It follows that the function $\boldsymbol{\zeta}^\star[\mathbf{z}(\mathbf{z}')]$ can be rewritten as $\boldsymbol{\zeta}^\star(\mathbf{z}')$, that is, in the form (A.2), by changing its coefficients $\mathbf{b}$ and $\mathbf{c}$ in $\mathbf{b}' = \mathbf{b}/r_c$ and $\mathbf{c}' = (\mathbf{c} - \mathbf{z}_c)/r_c$, respectively. For

this reason, it is sufficient to prove that the function (A.2) transforms the unit circle in another one, for $|\mathbf{c}| = c \neq 1$. This property is verified through the search for a point $\boldsymbol{\zeta}_c$ (the center of the transformed circle) and a positive constant ρ_c (its radius) such that the following equation (where the constant $\mathbf{d}$ stays for $\mathbf{c} - \mathbf{b}/(\mathbf{a} - \boldsymbol{\zeta}_c)$):

$$\rho_c^2 \equiv \left[\boldsymbol{\zeta}^\star(\mathbf{z}) - \boldsymbol{\zeta}_c\right]\left[\overline{\boldsymbol{\zeta}}^\star(\mathbf{z}) - \overline{\boldsymbol{\zeta}}_c\right] = (\mathbf{a} - \boldsymbol{\zeta}_c)\left(\overline{\mathbf{a}} - \overline{\boldsymbol{\zeta}}_c - \frac{\overline{\mathbf{b}}}{\overline{\mathbf{c}}}\right)\frac{(\mathbf{z} - \mathbf{d})(\mathbf{z} - 1/\overline{\mathbf{d}})}{(\mathbf{z} - \mathbf{c})(\mathbf{z} - 1/\overline{\mathbf{c}})}, \tag{A.3}$$

holds identically for any $\mathbf{z} \in \mathcal{C}$. In order to reach the independence of $\mathbf{z}$ of the third side, $\mathbf{d} = \mathbf{c}$ or $\mathbf{d} = 1/\overline{\mathbf{c}}$ must be assumed. But the first choice implies $\mathbf{b} = 0$, so that only the second one is really possible, leading to the following specification of the center and of the radius of the transformed circle $\boldsymbol{\zeta}^\star(\mathcal{C})$:

$$\boldsymbol{\zeta}_c = \mathbf{a} + \frac{\mathbf{b}\overline{\mathbf{c}}}{1 - c^2}, \qquad \rho_c = \frac{|\mathbf{b}|}{\left|1 - c^2\right|}. \tag{A.4}$$

In order to specify the above relation for the function (3.5), its values on the origin ($\boldsymbol{\zeta}_0^\star = \boldsymbol{\gamma}/\boldsymbol{\beta}$) and at infinity ($\boldsymbol{\zeta}_\infty^\star = \boldsymbol{\beta}/\boldsymbol{\alpha}$) are introduced, the coefficients $\mathbf{b}$ and $\mathbf{c}$ are changed in $\mathbf{b}/r_c$ and $\mathbf{c}/r_c$, and the relations between $\mathbf{a}$, $\mathbf{b}$, and $\mathbf{c}$ and the constants $\boldsymbol{\alpha}$, $\boldsymbol{\beta}$, and $\boldsymbol{\gamma}$ (3.3) are used. A circle $\mathcal{C}(r_c \mid 0)$ of radius $r_c \neq r^\star = \zeta_\infty^\star = \beta/\alpha$ and center on the origin $\mathbf{z}_c = 0$ of the $\mathbf{z}$-plane is mapped by the function $\boldsymbol{\zeta}^\star(\mathbf{z})$ (3.5) in another circle having center $\boldsymbol{\zeta}_c(r_c)$ on the point:

$$\boldsymbol{\zeta}_c(r_c) = \boldsymbol{\zeta}_0^\star + \frac{r_c^2}{r^{\star 2} - r_c^2}\left(\boldsymbol{\zeta}_0^\star - \boldsymbol{\zeta}_\infty^\star\right) = \boldsymbol{\zeta}_\infty^\star + \frac{r^{\star 2}}{r_c^2 - r^{\star 2}}\left(\boldsymbol{\zeta}_\infty^\star - \boldsymbol{\zeta}_0^\star\right), \tag{A.5}$$

the second side of which shows that this center moves from $\boldsymbol{\zeta}_0^\star$ to the infinity along the direction $\boldsymbol{\zeta}_0^\star - \boldsymbol{\zeta}_\infty^\star$ for r_c growing from 0 to the critical value $r^\star$. From the third side it follows that the center moves from the infinity to the point $\boldsymbol{\zeta}_\infty^\star$ along the direction $\boldsymbol{\zeta}_\infty^\star - \boldsymbol{\zeta}_0^\star$ when r_c runs from $r^\star$ to $+\infty$. this way, the center results to be external to the line joining the points $\boldsymbol{\zeta}_0^\star$ and $\boldsymbol{\zeta}_\infty^\star$ for any r_c. The radius of the image circle is given by

$$\rho_c(r_c) = \frac{r^\star r_c}{\left|r^{\star 2} - r_c^2\right|}\left|\boldsymbol{\zeta}_0^\star - \boldsymbol{\zeta}_\infty^\star\right|, \tag{A.6}$$

which results to be greater than the distance from the center and the point $\boldsymbol{\zeta}_0^\star$ for $r_c < r^\star$ and from the center and the point $\boldsymbol{\zeta}_\infty^\star$ for $r_c > r^\star$: all the circles cut the segment joining $\boldsymbol{\zeta}_0^\star$ with $\boldsymbol{\zeta}_\infty^\star$. Moreover, two circles $\boldsymbol{\zeta}^\star[\mathcal{C}(r_{c1} \mid 0)]$ and $\boldsymbol{\zeta}^\star[\mathcal{C}(r_{c2} \mid 0)]$ do not intersect if $r_{c1} \neq r_{c2}$.

In what curve the function (A.2) maps the unit circle for $c = 1$? By assuming $\mathbf{c} = \exp(\mathbf{i}\tau)$ and $\mathbf{z} = \exp(\mathbf{i}\theta)$ in the definition (A.2) one obtains

$$\boldsymbol{\zeta}^\star[\exp(\mathbf{i}\theta)] = \mathbf{a} - \frac{\mathbf{b}\overline{\mathbf{c}}}{2} - \mathbf{i}\frac{\mathbf{b}\overline{\mathbf{c}}}{2}\cot g\frac{\theta - \tau}{2}, \tag{A.7}$$

from which it appears that the circle is transformed in a straight line. By introducing the constants $\boldsymbol{\alpha}$, $\boldsymbol{\beta}$, and $\boldsymbol{\gamma}$ (3.3) inside **a**, **b**, and **c**, the above relation implies that the circle $\mathcal{C}(r^\star \mid 0)$ having the critical radius $r^\star$ is transformed by the function (3.5) in the straight line:

$$\boldsymbol{\zeta}^\star\left[r^\star \exp(\mathbf{i}\theta)\right] = \frac{1}{2}\left(\boldsymbol{\zeta}_0^\star + \boldsymbol{\zeta}_\infty^\star\right) - \frac{\mathbf{i}}{2}\left(\boldsymbol{\zeta}_\infty^\star - \boldsymbol{\zeta}_0^\star\right)\cot g\frac{\theta+\omega}{2}. \tag{A.8}$$

The line (A.8) is orthogonal to the segment joining $\boldsymbol{\zeta}_0^\star$ with $\boldsymbol{\zeta}_\infty^\star$ and it cuts that segment in its middle point $(\boldsymbol{\zeta}_0^\star + \boldsymbol{\zeta}_\infty^\star)/2$.

B. Position of the circle $\mathcal{C}^\star$ with respect to $\mathcal{C}$

In the present section, the relative position of the two circles $\mathcal{C}$ and $\mathcal{C}^\star$ is investigated, by showing that it depends on the constants α, β, and γ and on the phase difference $\nu = \omega - \chi$. For the sake of clearness, some issues about the position of the center $\boldsymbol{\zeta}_c(1)$ and of the radius $\rho_c(1)$ (3.6) of the transformed circle $\mathcal{C}^\star$ need to be preliminarily discussed. An important information about $\boldsymbol{\zeta}_c(1)$ concerns if it lies ($|\boldsymbol{\zeta}_c(1)| < 1$) or not ($|\boldsymbol{\zeta}_c(1)| > 1$) in $\mathring{\mathcal{C}}$. By accounting for that $|\boldsymbol{\zeta}_c(1)| = \beta R/|\beta^2 - \alpha^2|$, the modulus $|\boldsymbol{\zeta}_c(1)|$ holds 1 for $\beta = \beta_l(\alpha, \gamma \mid \nu)$ or for $\beta = \beta_u(\alpha, \gamma \mid \nu)$ with

$$\beta_l = \frac{1}{2}\left(\sqrt{R^2 + 4\alpha^2} - R\right) < \alpha, \qquad \beta_u = \frac{1}{2}\left(\sqrt{R^2 + 4\alpha^2} + R\right) > \alpha. \tag{B.1}$$

In terms of the above quantities, $|\boldsymbol{\zeta}_c(1)|$ results to be larger than 1 for $\beta_l < \beta < \beta_u$ and smaller for $\beta < \beta_l$ or $\beta > \beta_u$. About $\rho_c(1)$, it is larger than 1 for $\beta < \alpha < \gamma$ and smaller for $\alpha > \beta, \gamma$.

Our analysis of the relative positions between the two circles $\mathcal{C}$ and $\mathcal{C}^\star$ starts by searching the conditions in which $\mathcal{C}^\star$ lies inside $\mathcal{C}$. As stated above, it is needed that $\beta < \beta_l$ or $\beta > \beta_u$, so that $|\boldsymbol{\zeta}_c(1)| < 1$. In this hypothesis on β, the inequality $1 - |\boldsymbol{\zeta}_c(1)| > \rho_c(1)$ leads to the relation

$$\left(\alpha^2 - \beta^2\right)\left(\alpha^2 - \gamma^2\right) > 2\beta\left|\alpha^2 - \beta^2\right|R, \tag{B.2}$$

that is satisfied via the constraint (3.8) for $\alpha > \beta, \gamma$ or for $\alpha < \beta < \gamma$, but it can be shown that the second case cannot be verified. It follows that $\mathcal{C}^\star \subset \mathring{\mathcal{C}}$ when $\alpha > \beta, \gamma$ and $\beta < \beta_l$: the vortex is said to be of kind 1. Instead, the image circle $\mathcal{C}^\star$ is external and not including the unit circle $\mathcal{C}$ if $\alpha > \beta, \gamma$ and $\beta > \beta_l$ or if $\alpha < \beta, \gamma$ and $\beta < \beta_u$, the condition $|\boldsymbol{\zeta}_c(1)| - 1 > \rho_c(1)$ leading also in this case to the inequality (B.2) and $|\boldsymbol{\zeta}_c(1)| > 1$ implying $\beta_l < \beta < \beta_u$. However, it can be shown that the first case ($\alpha > \beta, \gamma$) cannot be verified. It follows that $\mathcal{C}^\star$ is external and not including $\mathcal{C}$ for $\alpha < \beta, \gamma$ and $\beta < \beta_u$: in this case the vortex is said to be of kind 3. Finally, the conditions to have the image circle $\mathcal{C}^\star$ including the unit one $\mathcal{C}$ are deduced by solving the inequality $\rho_c(1) > 1 + |\boldsymbol{\zeta}_c(1)|$, which can be rewritten as

$$\left(\alpha^2 - \beta^2\right)\left(\gamma^2 - \alpha^2\right) > 2\beta\left|\alpha^2 - \beta^2\right|R. \tag{B.3}$$

It is satisfied for $\beta < \alpha < \gamma$ by using the condition (3.8). The same condition inhibits the other possible solution $\gamma < \alpha < \beta$, because α and γ cannot be both smaller than β. It follows that $\mathcal{C}^\star$ is external and including $\mathcal{C}$ for $\beta < \alpha < \gamma$: in this case the vortex is said to be of kind 2.

C. Global behaviour of the map $\mathbf{z} \mapsto \boldsymbol{\zeta}^\star$

As summarized in Appendix A, the global behaviour of the map $\mathbf{z} \mapsto \boldsymbol{\zeta}^\star$ is easily understood by considering its action on a circle $\mathcal{C}(r_c \mid 0)$ with center on the origin and growing radius and by accounting for that the image of such a circle is still a circle with center in $\boldsymbol{\zeta}_c(r_c)$ (A.5) and radius $\rho_c(r_c)$ (A.6). For r_c growing from 0 to the critical value $r^\star = \beta/\alpha$, $\boldsymbol{\zeta}_c$ moves along the straight line passing through the points $\boldsymbol{\zeta}_0^\star$ and $\boldsymbol{\zeta}_\infty^\star$, r_0^∞ say, in direction $\boldsymbol{\zeta}_0^\star - \boldsymbol{\zeta}_\infty^\star$ from $\boldsymbol{\zeta}_0^\star$ ($r_c = 0$) to the infinity ($r_c \to r^\star$). At the same time, ρ_c grows from 0 ($r_c = 0$) to infinity ($r_c \to r^\star$). Indeed, the circle $\mathcal{C}(r^\star \mid 0)$ is mapped by the function $\mathbf{z} \mapsto \boldsymbol{\zeta}^\star$ in a straight line which is orthogonal to r_0^∞ and cuts the segment joining $\boldsymbol{\zeta}_0^\star$ with $\boldsymbol{\zeta}_\infty^\star$ in its middle point. When r_c grows above $r^\star$, the curve $\boldsymbol{\zeta}^\star[\mathcal{C}(r_c \mid 0)]$ becomes still a circle: $\boldsymbol{\zeta}_c$ moves on r_0^∞ always in direction $\boldsymbol{\zeta}_0^\star - \boldsymbol{\zeta}_\infty^\star$ from the infinity ($r_c \to r^\star$) to $\boldsymbol{\zeta}_\infty^\star$ ($r_c \to \infty$), while ρ_c decreases from the infinity ($r_c \to r^\star$) to 0 ($r_c \to \infty$). The behaviour of the map $\mathbf{z} \mapsto \boldsymbol{\zeta}^\star$ is now specified on the basis of the classification with respect to the first property.

A vortex of kind 1 has $r^\star < 1$ (see Table 1) and its corresponding set $\mathcal{A}$ does not fill the whole $\mathring{\mathcal{C}}$. The image of each circle $\mathcal{C}(r_c \mid 0)$ with $r_c < 1$ goes outside $\mathcal{C}^\star$ through the map $\mathbf{z} \mapsto \boldsymbol{\zeta}^\star$, even if its position is still not known with respect to $\mathcal{A}$. It can be deduced as follows. With the circle $\mathcal{C}^\star$ lying inside the unitary one, select an arbitrary radius r_c (in case, it approaches the unity from below) such that $\mathcal{C}(r_c \mid 0) \subset \mathcal{A}$. The image of $\mathcal{C}(r_c \mid 0)$ through the map $\mathbf{z} \mapsto \boldsymbol{\zeta}^\star$ cannot lie outside $\mathcal{C}$, because for $r_c \to 1^-$ it goes on $\mathcal{C}^\star \subset \mathring{\mathcal{C}}$. Moreover, it cannot intersect $\mathcal{C}$ (or $\mathcal{C}^\star$). Indeed, suppose that two intersection points exist. For the map $\mathbf{z} \mapsto \boldsymbol{\zeta}^\star$ is self-inverse (see Appendix A) and $\boldsymbol{\zeta}^\star(\mathcal{C}) = \mathcal{C}^\star$, it means that these points come from two points of the $\mathbf{z}$-plane lying on $\mathcal{C}^\star$ (or $\mathcal{C}$), which is absurd. As a consequence, the image of the circle $\mathcal{C}(r_c \mid 0)$ still lies in $\mathcal{A}$. It follows that $\mathcal{A}$ is mapped onto itself, while $\mathring{\mathcal{C}}^\star$ goes onto the outside of $\mathcal{C}$. For this reason, a circle $\mathcal{C}(r_c \mid 0)$ with $r_c < 1$ and $r_c \neq r^\star$ that intersects $\mathcal{C}^\star$ is mapped in a circle which has an arc inside $\mathcal{C}$, the complementary one outside $\mathcal{C}$, and does not intersect $\mathcal{C}^\star$. The arc inside $\mathcal{C}$ is the image of the arc of $\mathcal{C}(r_c \mid 0)$ that lies outside $\mathcal{C}^\star$, while the arc lying outside $\mathcal{C}$ is the image of the arc inside $\mathcal{C}^\star$.

Consider now a vortex of kind 2, for which (see Table 1) $r^\star < 1$. The set $\mathcal{A} = \mathring{\mathcal{C}}$ goes in that case onto the outside of the circle $\mathcal{C}^\star$. Indeed, the other possibility ($\boldsymbol{\zeta}^\star(\mathcal{A}) = \mathring{\mathcal{C}}^\star$) cannot occur, because for $r_c \to r^\star < 1$ the image of $\mathcal{C}(r_c \mid 0)$ through the map $\mathbf{z} \mapsto \boldsymbol{\zeta}^\star$ does not remain bounded. As a consequence, $\mathfrak{D}$ is mapped onto itself. Finally, a vortex of kind 3 has $r^\star > 1$ (see Table 1): its corresponding set $\mathcal{A} = \mathring{\mathcal{C}}$ goes onto the inside of $\mathcal{C}^\star$, for the same reason about the behaviour of $\mathbf{z} \mapsto \boldsymbol{\zeta}^\star$ in a neighbourhood of the critical radius. Also in this case, $\mathfrak{D}$ is mapped onto itself.

D. Invariant circle tangent to $\mathcal{C}$ and $\mathcal{C}^\star$

In the present appendix, the values of the parameter t for invariant circles (3.9) tangent to both $\mathcal{C}$ and $\mathcal{C}^\star$ are calculated: they are needed in order to define a branch of the inverse map $\mathbf{x} \mapsto \mathbf{z}$.

D.1. Invariant circle tangent to $\mathcal{C}$

Consider an invariant circle $\mathcal{C}_i(t)$ which is also tangent to $\mathcal{C}$. That invariant circle can lie inside $\mathcal{C}$ (I) or outside it, in this latter case $\mathcal{C}_i(t)$ can include (II) or not (III) the unit circle. At this

stage, one does not know which case among the above ones holds. The position $\mathbf{z}_i$ of its center and its radius r_i satisfy one of the following relations:

$$\left|\mathbf{z}_i(t) - 0\right| = \begin{cases} \mp\left[r_i(t) - 1\right] & - : I,\ + : II, \\ r_i(t) + 1 & III. \end{cases} \tag{D.1}$$

Due to the form (3.9) of the functions $\mathbf{z}_i$ and r_i, it is convenient to evaluate the quantity $\overline{\boldsymbol{\beta}}^2\boldsymbol{\delta}^2 = \beta^2(\alpha\gamma\exp(\mathbf{i}\nu) - \beta^2)$ and then to calculate the square $\left(\overline{\boldsymbol{\beta}}\boldsymbol{\delta} + \boldsymbol{\beta}\overline{\boldsymbol{\delta}}\right)^2$. In this way, by selecting the branch of $\boldsymbol{\delta}$ (square root of $\boldsymbol{\alpha}\boldsymbol{\gamma} - \boldsymbol{\beta}^2$) such that $\overline{\boldsymbol{\beta}}\boldsymbol{\delta} + \boldsymbol{\beta}\overline{\boldsymbol{\delta}} \geq 0$, one obtains

$$\overline{\boldsymbol{\beta}}\boldsymbol{\delta} + \boldsymbol{\beta}\overline{\boldsymbol{\delta}} = \sqrt{2}\beta S, \tag{D.2}$$

with S being the positive root of $\delta^2 + \alpha\gamma\cos\nu - \beta^2$. The definition of center and radius (3.9) of the invariant circle, together with the relation (D.2) are inserted in (D.1), so that the following equation in the parameter t is obtained:

$$\underbrace{\alpha^2 - \beta^2 + \delta^2}_{p} - \underbrace{\sqrt{2}\beta S t}_{q} = \pm\underbrace{2\alpha\delta}_{s}\sqrt{t^2 + 1}, \tag{D.3}$$

where the upper sign holds in the cases I and II and the lower one when $\mathcal{C}_i(t)$ is external and not including $\mathcal{C}(III)$. The above equation has the following two real solutions:

$$\frac{-\beta\left(\alpha^2 - \beta^2 + \delta^2\right)S \pm \sqrt{2}\alpha^2\delta\sqrt{\alpha^2 + \gamma^2 - 2\left(\beta^2 + \delta^2\right)}}{\sqrt{2}\left(2\alpha^2\delta^2 - \beta^2 S^2\right)}, \tag{D.4}$$

which are called t_1 and t_2 (with $t_2 < t_1$): as a consequence t must be equal to t_1 or to t_2. Moreover, the sign of the quantity $\alpha^2 - \beta^2 + \delta^2 - \sqrt{2}\beta S t$ (D.3) specifies if the circle is in the conditions I, II (it is positive) or III (negative) and a calculation of r_i (if needed) discriminates between the cases I ($r_i < 1$) or II ($r_i > 1$).

D.2. Invariant circle tangent to $\mathcal{C}^\star$

Consider now another invariant circle $\mathcal{C}_i(t)$ which is also tangent to $\mathcal{C}^\star$. The same relations (D.1) hold, with $\boldsymbol{\zeta}_c(1)$ in place of 0 in the left-hand side and $\rho_c(1)$ in place of 1 in the right one. As before, the first row holds for $\mathcal{C}_i$ inside $\mathcal{C}^\star$ (sign −, condition I) or outside $\mathcal{C}^\star$ (sign +, condition II), while the second row holds for the invariant circle external and not including $\mathcal{C}^\star$. By using the forms (3.9), (3.6) of the position of the center and of the radius of the invariant circle ($\mathbf{z}_i$ and r_i) and of $\mathcal{C}^\star$ ($\boldsymbol{\zeta}_c(1)$ and $\rho_c(1)$), the following equation in t:

$$\alpha^2 - \beta^2 + \delta^2 - \sqrt{2}\beta S t = \pm 2\frac{\alpha^2 - \beta^2}{\left|\alpha^2 - \beta^2\right|}\alpha\delta\sqrt{t^2 + 1}, \tag{D.5}$$

is obtained. As before, the upper sign holds in the conditions I and II, while the lower one must be selected in the condition III. Notice that (D.5) is identical to the one (D.3) for vortices

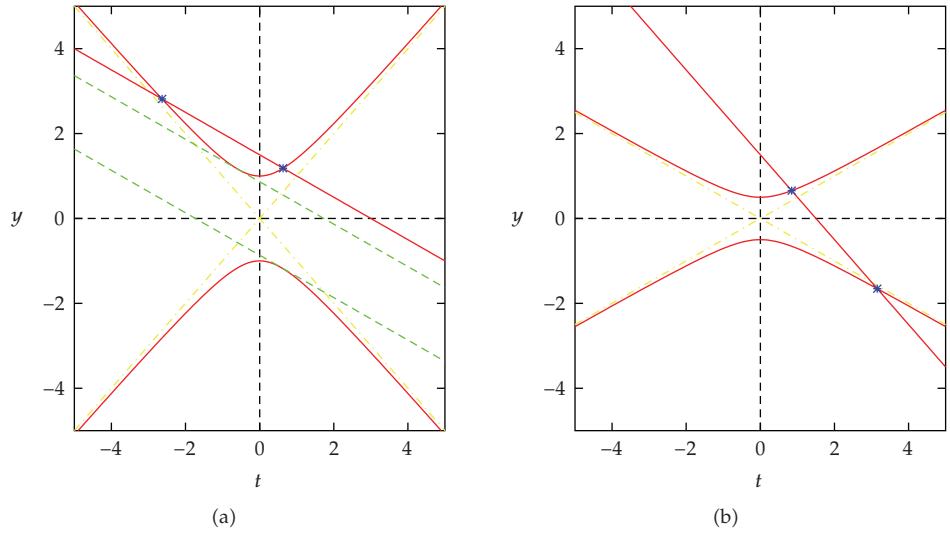

Figure 10: Functions $y = \pm s\sqrt{t^2+1}$ (red lines), their asymptotes (yellow), and the straight line $y = p - qt$ (red) versus t, for (a) $p = 1.5$, $q = 0.5 < s = 1$ and (b) $q = 1 > s = 0.5$. In (a) also the tangent lines at $p = \pm\sqrt{s^2 - q^2}$ are drawn with green lines. Intersection points are marked with blue symbols.

of kind 1 or 2 with respect to the first property ($\alpha > \beta$), while its right-hand side has opposite sign for vortices of kind 3 ($\alpha < \beta$).

D.3. Position of $\mathcal{C}_i(t)$ with respect to $\mathcal{C}$ and $\mathcal{C}^\star$

At this stage, the following key remark is needed: the circle $\mathcal{C}^\star$ is the image through the map $\mathbf{z} \mapsto \boldsymbol{\zeta}^\star$ of the unit one $\mathcal{C}$, so that if an invariant circle is tangent to $\mathcal{C}$, it must be also tangent to $\mathcal{C}^\star$. For this reason, some of the previous possibilities (labeled with I, II, and III) must be ruled out, once the relative position of $\mathcal{C}^\star$ with respect to $\mathcal{C}$ is known. The invariant circle lies inside $\mathcal{C}$ and includes $\mathcal{C}^\star$ for vortices of kind 1 with respect to the first property: the right-hand side of (D.3) is positive. The same holds for vortices of kind 2: $\mathcal{C}_i$ lies inside $\mathcal{C}^\star$ and includes $\mathcal{C}$. For vortices of kind 3, the signs in the right-hand sides of (D.3), (D.5) are necessarily different, being $(\alpha^2 - \beta^2)/|\alpha^2 - \beta^2| = -1$. In this way, if the invariant circle includes $\mathcal{C}$, it is also external to $\mathcal{C}^\star$, or, on the contrary, if it includes $\mathcal{C}^\star$, it lies also outside $\mathcal{C}$: the tangent $\mathcal{C}_i$ cannot include both circles $\mathcal{C}$ and $\mathcal{C}^\star$ or lie outside them, at the same time.

Another way to understand this behaviour is based on the discussion of (D.3), rewritten for the sake of shortness as $p - qt = \pm s(t^2+1)^{1/2}$ with $p = \alpha^2 - \beta^2 + \delta^2$, $q = 2\beta\delta\cos\mu > 0$ and $s = 2\alpha\delta > 0$. It defines the intersection points between the straight line $y = p - qt$ and the two curves $y = \pm s(t^2+1)^{1/2}$ in a plane (t, y), as shown in Figure 10. Two conditions must be considered, as discussed below. If $q < s$, solutions exist only for $p \geq (s^2 - q^2)^{1/2}$ ($p \leq -(s^2 - q^2)^{1/2}$): they stay both above (below) the axis t, so that only the positive (negative) sign holds in the right-hand side of (D.3). On the contrary, if $q \geq s$, the intersection points always exist: one lies on the curve $y = +s(t^2+1)^{1/2}$ and the other one on $y = -s(t^2+1)^{1/2}$ (for $q = s$ and $p = 0$ the values $t = \pm\infty$ are obtained). Vortices of kinds 1 and 2 with respect to the first

property satisfy this condition, having $q < s$ and $p \geq (s^2 - q^2)^{1/2}$. Moreover, from the latter condition, it follows that the right-hand side of (D.3) must be taken positive, as shown also above. Vortices of kind 3 can verify the first ($q < s$) or the second ($q \geq s$) of the above conditions, depending on the positions of the poles $\mathbf{z}_1$ and $\mathbf{z}_2$ and on the ratio $\mathbf{a}_2/\mathbf{a}_1$ in the Schwarz function (3.1).

D.4. Choice of the parameter t

The last issue to be discussed concerns the choice of an invariant circle which neither intersects $\mathcal{C}$ nor $\mathcal{C}^\star$. This choice is based on the values t_1 and t_2 of the parameter t given in (D.4), which correspond to invariant circles that are tangent to $\mathcal{C}$ and $\mathcal{C}^\star$, and on the position of the straight line $y = p - qt$ relative to the curves $y = \pm s(t^2+1)^{1/2}$.

As discussed before, a vortex of kind 1 with respect to the first property has $\mathcal{C}_i \subset \mathring{\mathcal{C}}$ and $\mathcal{C}^\star \subset \mathring{\mathcal{C}}_i$, while for a vortex of kind 2 the relations $\mathcal{C} \subset \mathring{\mathcal{C}}_i$ and $\mathcal{C}_i \subset \mathring{\mathcal{C}}^\star$ are verified. In both the above cases, the inequality $p - qt > s(t^2+1)^{1/2}$ follows (see Figure 10(a)): it is verified for any $t \in (t_1, t_2)$ and, in particular, for the mean $(t_1 + t_2)/2$, which is the value of the parameter t adopted in the paper. As a consequence, the branch of the inverse map $\mathbf{x} \mapsto \mathbf{z}$ used for vortices of kind 1 satisfies for any $\mathbf{x}$ the inequality $|\mathbf{z}(\mathbf{x}) - \mathbf{z}_i| > r_i$, while the branch for vortices of kind 2 verifies the inequality $|\mathbf{z}(\mathbf{x}) - \mathbf{z}_i| < r_i$.

Consider now the vortices which are of kind 3 with respect to the first property. If $q < s$ and $p \geq (s^2 - q^2)^{1/2}$, the roots (D.4) verify (D.3) with the upper sign: both circles $\mathcal{C}_i(t_1)$, $\mathcal{C}_i(t_2)$ include $\mathcal{C}$. Moreover, $p - qt > s(t^2+1)^{1/2}$ for any t belonging to the interval (t_1, t_2), as shown in Figure 10(a). In the same interval, the inequality $|\boldsymbol{\zeta}_i - \boldsymbol{\zeta}_c(1)| > \rho_i + \rho_c(1)$ is verified: any invariant circle $\mathcal{C}_i(t)$, with $t \in (t_1, t_2)$, includes $\mathcal{C}$ and does not intersect $\mathcal{C}^\star$. As before, the mean value $(t_1 + t_2)/2$ of the parameter t is selected and the corresponding branch of the inverse satisfies the inequality $|\mathbf{z}(\mathbf{x}) - \mathbf{z}_i| < r_i$, for any $\mathbf{x}$. If $q < s$ and $p \leq -(s^2 - q^2)^{1/2}$, the roots (D.4) verify (D.3) with the lower sign: both circles $\mathcal{C}_i(t_1)$ and $\mathcal{C}_i(t_2)$ include $\mathcal{C}^\star$. The inequality $p - qt < -s(t^2+1)^{1/2}$ is also verified for any $t \in (t_1, t_2)$, it follows that $|\boldsymbol{\zeta}_i - 0| > 1 + r_i$, so that each invariant circle $\mathcal{C}_i$ does not intersect $\mathcal{C}$. The mean value of the parameters t_1 and t_2 is still adopted and the corresponding branch of the inverse verifies the inequality $|\mathbf{z}(\mathbf{x}) - \mathbf{z}_i| > r_i$, for any $\mathbf{x}$. Finally, consider the vortices such that $q \geq s$, having $p - qt_1 > 0$ and $p - qt_2 < 0$. The invariant circle $\mathcal{C}_i(t_1)$ includes $\mathcal{C}$, while the other one $\mathcal{C}_i(t_2)$ includes $\mathcal{C}^\star$. Moreover, $p - qt > s(t^2+1)^{1/2}$ for any $t < t_1$ and $p - qt < -s(t^2+1)^{1/2}$ for any $t > t_2$ (see Figure 10(b)): as a consequence, the inequalities $|\boldsymbol{\zeta}_i - \boldsymbol{\zeta}_c(1)| > \rho_i + \rho_c(1)$ for $t < t_1$ and $|\mathbf{z}_i - 0| > 1 + r_i$ for $t > t_2$ hold. In the first case, ($t < t_1$) $\mathcal{C}_i(t)$ includes $\mathcal{C}$ and does not intersect $\mathcal{C}^\star$, while in the other range of the parameter ($t > t_2$) $\mathcal{C}_i$ includes $\mathcal{C}^\star$ and does not intersect $\mathcal{C}$. In the paper, the value $2t_1 - t_2 < t_1$ of the parameter t is adopted, leading to a branch of the inverse map which satisfies the inequality $|\mathbf{z}(\mathbf{x}) - \mathbf{z}_i| < r_i$, for any $\mathbf{x}$.

E. Some properties of the map $\mathbf{z} \mapsto \mathbf{x}$

In the present appendix, the conditions under which the function $\mathbf{x}(\mathbf{z})$ (3.2) maps the points of a given circle $\mathbf{z} = \mathbf{z}_0 + r\boldsymbol{\zeta}$ for $\boldsymbol{\zeta} \in \mathcal{C}$ ($\mathbf{z}_0$ is the center and r the radius) in points lying on another circle (with center on $\mathbf{x}_0$ and radius R_0) are investigated. The map $\mathbf{z} \mapsto \mathbf{x}$ has the form

$$\mathbf{x}(\mathbf{z}) = \mathbf{a} + \frac{\mathbf{b}}{\mathbf{z} - \mathbf{p}} + \frac{\mathbf{c}}{\mathbf{z} - \mathbf{q}}, \tag{E.1}$$

with $\mathbf{a}$, $\mathbf{b}$, $\mathbf{c}$, $\mathbf{p}$, $\mathbf{q}$ being complex constants. Conditions among the coefficients $\mathbf{b}$, $\mathbf{c}$, the rescaled ones $\mathbf{p}_r = \mathbf{p} - \mathbf{z}_0$, $\mathbf{q}_r = \mathbf{q} - \mathbf{z}_0$ and the radius r (which is assumed different from p_r and q_r) have to be specified. As it results from the following analysis, the center $\mathbf{x}_0$ and the radius R_0 of the image circle will be also defined.

In order to map points of the circle $\mathbf{z} = \mathbf{z}_0 + r\boldsymbol{\zeta}$ in points on another circle, the quantity

$$\left[\mathbf{x}(\boldsymbol{\zeta}) - \mathbf{x}_0\right]\left[\overline{\mathbf{x}}(\boldsymbol{\zeta}) - \overline{\mathbf{x}}_0\right] = \mathbf{a}_r\left[\overline{\mathbf{x}}(\mathbf{z}_0) - \overline{\mathbf{x}}_0\right]\frac{\mathbf{P}_1(\boldsymbol{\zeta})}{(\boldsymbol{\zeta} - \mathbf{p}_r/r)(\boldsymbol{\zeta} - \mathbf{q}_r/r)}\frac{\mathbf{P}_2(\boldsymbol{\zeta})}{(\boldsymbol{\zeta} - r/\overline{\mathbf{p}}_r)(\boldsymbol{\zeta} - r/\overline{\mathbf{q}}_r)} \tag{E.2}$$

must be (positive and) independent of the position $\boldsymbol{\zeta}$. In (E.2), the rescaled coefficient $\mathbf{a}_r$ is also used, with $\mathbf{a}_r$ being defined as $\mathbf{a} - \mathbf{x}_0$. The functions $\mathbf{P}_1$ and $\mathbf{P}_2$ are the following polynomials of second degree in $\boldsymbol{\zeta}$:

$$\begin{aligned}
\mathbf{P}_1(\boldsymbol{\zeta}) &= \boldsymbol{\zeta}^2 + \frac{1}{r}\left[\frac{\mathbf{b}+\mathbf{c}}{\mathbf{a}_r} - (\mathbf{p}_r + \mathbf{q}_r)\right]\boldsymbol{\zeta} + \frac{1}{r^2}\left(\mathbf{p}_r\mathbf{q}_r - \frac{\mathbf{b}\mathbf{q}_r + \mathbf{c}\mathbf{p}_r}{\mathbf{a}_r}\right),\\
\mathbf{P}_2(\boldsymbol{\zeta}) &= \boldsymbol{\zeta}^2 + r\frac{\overline{\mathbf{b}} + \overline{\mathbf{c}} - \overline{\mathbf{a}}_r(\overline{\mathbf{p}}_r + \overline{\mathbf{q}}_r)}{\overline{\mathbf{a}}_r\overline{\mathbf{p}}_r\overline{\mathbf{q}}_r - \overline{\mathbf{b}}\overline{\mathbf{q}}_r - \overline{\mathbf{c}}\,\overline{\mathbf{p}}_r}\boldsymbol{\zeta} + \frac{r^2\overline{\mathbf{a}}_r}{\overline{\mathbf{a}}_r\overline{\mathbf{p}}_r\overline{\mathbf{q}}_r - \overline{\mathbf{b}}\overline{\mathbf{q}}_r - \overline{\mathbf{c}}\,\overline{\mathbf{p}}_r}.
\end{aligned} \tag{E.3}$$

The right-hand side of (E.2) results to be independent of $\boldsymbol{\zeta}$ if the zeros of the polynomial $\mathbf{P}_1$ are in $r/\overline{\mathbf{p}}_r$, $r/\overline{\mathbf{q}}_r$ and the ones of the polynomial $\mathbf{P}_2$ in $\mathbf{p}_r/r$, $\mathbf{q}_r/r$. In terms of the quantity $\boldsymbol{\eta}_r = \mathbf{p}_r\overline{\mathbf{q}}_r$, these conditions on $\mathbf{P}_1$ and $\mathbf{P}_2$ lead to the following two relations:

$$\mathbf{a}_r = -\overline{\mathbf{p}}_r\left(\frac{\mathbf{b}}{r^2 - p_r^2} + \frac{\mathbf{c}}{r^2 - \overline{\boldsymbol{\eta}}_r}\right) = -\overline{\mathbf{q}}_r\left(\frac{\mathbf{b}}{r^2 - \boldsymbol{\eta}_r} + \frac{\mathbf{c}}{r^2 - q_r^2}\right), \tag{E.4}$$

with the condition $\mathbf{P}_1(r/\overline{\mathbf{p}}_r) = 0$ giving the same coefficient $\mathbf{a}_r$ as the one $\overline{\mathbf{P}}_2(\mathbf{p}_r/r) = 0$, as it occurs for $\mathbf{P}_1(r/\overline{\mathbf{q}}_r) = \overline{\mathbf{P}}_2(\mathbf{q}_r/r) = 0$. The last two sides in the above formula give a constraint on the center $\mathbf{z}_0$ (through the quantities $\mathbf{p}_r$ and $\mathbf{q}_r$) and the radius r of the circle in the $\mathbf{z}$-plane. By conjugating both sides of the following equation in r^2:

$$\frac{\mathbf{b}\overline{\mathbf{q}}_r}{r^2 - \boldsymbol{\eta}_r} - \frac{\mathbf{c}\overline{\mathbf{p}}_r}{r^2 - \overline{\boldsymbol{\eta}}_r} = \frac{\mathbf{b}\overline{\mathbf{p}}_r}{r^2 - p_r^2} - \frac{\mathbf{c}\overline{\mathbf{q}}_r}{r^2 - q_r^2}, \tag{E.5}$$

a linear system in $1/(r^2 - \boldsymbol{\eta}_r)$ and $1/(r^2 - \overline{\boldsymbol{\eta}}_r)$ is obtained, the solution of which implies that the following complex quantity:

$$\frac{\mathbf{d}_1 q_r^2 + \mathbf{d}_2 p_r^2}{\mathbf{d}_1 + \mathbf{d}_2}, \tag{E.6}$$

must be real and positive, with $\mathbf{d}_1 = \overline{\mathbf{b}}(\overline{\mathbf{p}} - \overline{\mathbf{q}})(\mathbf{c}\mathbf{p}_r + \mathbf{b}\mathbf{q}_r)$ and $\mathbf{d}_2 = \mathbf{c}(\mathbf{p} - \mathbf{q})(\overline{\mathbf{c}}\,\overline{\mathbf{p}}_r + \overline{\mathbf{b}}\overline{\mathbf{q}}_r)$. Moreover, the squared radius r^2 must also be equal to the above quantity. The quantity (E.6) must be real and positive, or $\mathbf{d}_1$ is not parallel to $\mathbf{d}_2$ and $p_r = q_r$, or $\mathbf{d}_1$ is parallel to $\mathbf{d}_2$. The first case is not possible: it implies $r = p_r = q_r$ and the corresponding quantity $\mathbf{a}_r$ (E.4) becomes singular.

It follows that $\mathbf{d}_1$ must be parallel to $\mathbf{d}_2$. Hereafter, d_1' and d_2' will indicate the components of $\mathbf{d}_1$ and $\mathbf{d}_2$ in direction of their sum $\mathbf{d}_1 + \mathbf{d}_2$. Apices are needed to distinguish d_k' $(k = 1, 2)$ by $|\mathbf{d}_k| = d_k$: actually d_k' may be $+d_k$ or $-d_k$, if the difference between the arguments of $\mathbf{d}_k$ and of $\mathbf{d}_1 + \mathbf{d}_2$ vanishes or holds $\pm\pi$, respectively. Real quantities d_1' and d_2' depend on the parameters in (E.1) by the relations $d_1' = |\mathbf{p} - \mathbf{q}||\mathbf{b}\mathbf{q}_r + \mathbf{c}\mathbf{p}_r|b'$ (with the above convection on the apex) and $d_2' = |\mathbf{p} - \mathbf{q}||\mathbf{b}\mathbf{q}_r + \mathbf{c}\mathbf{p}_r|c'$. Then the radius r must satisfy the relation:

$$r^2 = \frac{d_1' q_r^2 + d_2' p_r^2}{d_1' + d_2'} \tag{E.7}$$

which leads through the forms of $\mathbf{a}_r$ (E.4) to the position of the center of the image circle:

$$\mathbf{x}_0 = \mathbf{a} - \mathbf{a}_r = \mathbf{a} + \frac{(b' + c')^2}{(q_r^2 - p_r^2)(b^2 q_r^2 - c^2 p_r^2)} \overline{\mathbf{p}}_r \overline{\mathbf{q}}_r (\mathbf{b}\mathbf{q}_r + \mathbf{c}\mathbf{p}_r), \tag{E.8}$$

as well as to its radius:

$$R_0 = \left[\mathbf{a}_r \left(\overline{\mathbf{a}}_r - \frac{\overline{\mathbf{b}}}{\overline{\mathbf{p}}_r} - \frac{\overline{\mathbf{c}}}{\overline{\mathbf{q}}_r} \right) \right]^{1/2} = \frac{|b' + c'||b' q_r^2 + c' p_r^2|}{|q_r^2 - p_r^2||b^2 q_r^2 - c^2 p_r^2|} |\mathbf{b}\mathbf{q}_r + \mathbf{c}\mathbf{p}_r|. \tag{E.9}$$

In the present case, we have to consider the images through the map $\mathbf{z} \mapsto \mathbf{x}$ of the circles of the first family. The center position $\mathbf{z}_0$ assumes the value $\mathbf{z}_i(t)$ (3.9) and $\mathbf{p}_r$ and $\mathbf{q}_r$ become

$$\mathbf{p}_r = \frac{\mathbf{w}_1 - \mathbf{w}_2}{\boldsymbol{\varepsilon}_1^2 + \boldsymbol{\varepsilon}_2^2} \boldsymbol{\varepsilon}_1 (\boldsymbol{\varepsilon}_1 - t\boldsymbol{\varepsilon}_2), \qquad \mathbf{q}_r = -\frac{\mathbf{w}_1 - \mathbf{w}_2}{\boldsymbol{\varepsilon}_1^2 + \boldsymbol{\varepsilon}_2^2} \boldsymbol{\varepsilon}_2 (\boldsymbol{\varepsilon}_2 + t\boldsymbol{\varepsilon}_1), \tag{E.10}$$

by using the quantities (6.1). As discussed before, the vectors $\mathbf{d}_1$ and $\mathbf{d}_2$ must be parallel. Indeed, a direct computation by using the quantities (E.10) gives

$$\mathbf{d}_1 = -|\mathbf{w}_1 - \mathbf{w}_2|^2 w_1^2 a_1 \overline{\boldsymbol{\varepsilon}}_1 \boldsymbol{\varepsilon}_2 t, \qquad \mathbf{d}_2 = -|\mathbf{w}_1 - \mathbf{w}_2|^2 w_2^2 a_2 \overline{\boldsymbol{\varepsilon}}_1 \boldsymbol{\varepsilon}_2 t \tag{E.11}$$

which shows that $\mathbf{d}_1$ and $\mathbf{d}_2$ have just the same argument $(d_1' = d_1, d_2' = d_2)$. The use of (E.10) and (E.11) into the constraint for r (E.6) leads to the radius $r = r_i(t)$ (3.9) of a circle of the first family (a similar behaviour is found also for each invariant circle of the second family, having center on the point $\mathbf{z}_{io}(t)$ $(|t| \geq 1)$: equation (E.7) still gives the corresponding radius $r = r_{io}(t)$ (3.10)) with parameter t. It follows that points on an invariant circle of the first family goes with the map $\mathbf{z} \mapsto \mathbf{x}$ on another circle in the physical plane. By using the real quantities $\varepsilon' = \boldsymbol{\varepsilon}_1 \overline{\boldsymbol{\varepsilon}}_2 + \overline{\boldsymbol{\varepsilon}}_1 \boldsymbol{\varepsilon}_2$, $\varepsilon'' = \varepsilon_1^2 - \varepsilon_2^2$, it is found that the center of such a circle lies on the point (E.8):

$$\mathbf{x}_i = -\boldsymbol{\beta}' - \frac{\boldsymbol{\alpha}^2}{\mathbf{w}_1 - \mathbf{w}_2} \frac{(\overline{\boldsymbol{\varepsilon}}_1 - \overline{\boldsymbol{\varepsilon}}_2 t)(\overline{\boldsymbol{\varepsilon}}_2 + \overline{\boldsymbol{\varepsilon}}_1 t)}{(\varepsilon' t - \varepsilon'')(\varepsilon'' t + \varepsilon')}. \tag{E.12}$$

In order to obtain a more useful form of the position of the center, the conjugates $\overline{\boldsymbol{\varepsilon}}_1$ and $\overline{\boldsymbol{\varepsilon}}_2$ are written in terms of the corresponding quantities $\boldsymbol{\varepsilon}_1$ and $\boldsymbol{\varepsilon}_2$ from the definitions of ε' and ε'', so that the above form of the position of the center becomes

$$\mathbf{x}_i(t) = \frac{\mathbf{x}_{io}^{+} + \mathbf{x}_{io}^{-}}{2} + \mathbf{i}\frac{\mathbf{x}_{io}^{-} - \mathbf{x}_{io}^{+}}{4}\left[f(t) - \frac{1}{f(t)}\right], \tag{E.13}$$

where the function f has the following form:

$$f(t) = \frac{\varepsilon' t - \varepsilon''}{\varepsilon'' t + \varepsilon'}. \tag{E.14}$$

Finally, the radius (E.9) of the image circle is written as

$$R_i(t) = \frac{\left|\mathbf{x}_{io}^{-} - \mathbf{x}_{io}^{+}\right|}{4}\left[|f(t)| + \frac{1}{|f(t)|}\right]. \tag{E.15}$$

Acknowledgments

The second author acknowledges the support of the Ph.D. in "*Scienze e tecnologie aerospaziali*" of the Second University of Naples. The authors acknowledge an anonymous reviewer for his helpful suggestions, which have deeply enhanced this work.

References

[1] P. G. Saffman, *Vortex Dynamics*, Cambridge Monographs on Mechanics and Applied Mathematics, Cambridge University Press, New York, NY, USA, 1992.
[2] P. J. Davis, *The Schwarz Function and Its Applications*, The Carus Mathematical Monographs, no. 17, The Mathematical Association of America, Washington, DC, USA, 1974.
[3] J. R. Kamm, *Shape and stability of two-dimensional uniform vorticity regions*, Ph.D. thesis, California Institute of Technology, Pasadena, Calif, USA, 1987.
[4] G. Riccardi, "Intrinsic dynamics of the boundary of a two-dimensional uniform vortex," *Journal of Engineering Mathematics*, vol. 50, no. 1, pp. 51–74, 2004.
[5] D. Crowdy, "A class of exact multipolar vortices," *Physics of Fluids*, vol. 11, no. 9, pp. 2556–2564, 1999.
[6] D. Crowdy, "Multipolar vortices and algebraic curves," *Proceedings of the Royal Society of London. Series A*, vol. 457, no. 2014, pp. 2337–2359, 2001.
[7] D. Crowdy and M. Cloke, "Stability analysis of a class of two-dimensional multipolar vortex equilibria," *Physics of Fluids*, vol. 14, no. 6, pp. 1862–1876, 2002.
[8] D. Crowdy, "The construction of exact multipolar equilibria of the two-dimensional Euler equations," *Physics of Fluids*, vol. 14, no. 1, pp. 257–267, 2002.
[9] D. Crowdy, "Exact solutions for rotating vortex arrays with finite-area cores," *Journal of Fluid Mechanics*, vol. 469, pp. 209–235, 2002.
[10] D. Crowdy and J. Marshall, "Growing vortex patches," *Physics of Fluids*, vol. 16, no. 8, pp. 3122–3130, 2004.
[11] H. Aref and D. L. Vainchtein, "Point vortices exhibit asymmetric equilibria," *Nature*, vol. 392, no. 6678, pp. 769–770, 1998.
[12] D. Crowdy and J. Marshall, "Analytical solutions for rotating vortex arrays involving multiple vortex patches," *Journal of Fluid Mechanics*, vol. 523, pp. 307–337, 2005.
[13] I. Gned, D. Durante, G. Riccardi, and L. Zannetti, "The self-induced dynamics of vortex patches," in *Proceedings of IUTAM Symposium on 150 Years of Vortex Dynamics*, Lyngby, Denmark, October 2008.
[14] N. J. Zabusky, M. H. Hughes, and K. V. Roberts, "Contour dynamics for the Euler equations in two dimensions," *Journal of Computational Physics*, vol. 30, no. 1, pp. 96–106, 1979.

[15] D. G. Dritschel, "Contour dynamics and contour surgery: numerical algorithms for extended, high-resolution modelling of vortex dynamics in two-dimensional, inviscid, incompressible flows," *Computer Physics Reports*, vol. 10, no. 3, pp. 77–146, 1989.
[16] D. I. Pullin, "Contour dynamics methods," *Annual Review of Fluid Mechanics*, vol. 24, pp. 89–115, 1992.
[17] M. V. Melander, J. C. McWilliams, and N. J. Zabusky, "Axisymmetrization and vorticity-gradient intensification of an isolated two-dimensional vortex through filamentation," *Journal of Fluid Mechanics*, vol. 178, pp. 137–159, 1987.